Faculdade de Engenharia da Universidade do Porto

Antibiotic Free Nano/Microparticles to Fight *Helicobacter pylori*

Ana Moura

Dissertação realizada no âmbito do
Mestrado em Engenharia Biomédica

Orientador: M. Cristina L. Martins (INEB/i3S)
Co-orientador: Paula Parreira (INEB/i3S)

Setembro 2018

U.PORTO
FEUP FACULDADE DE ENGENHARIA UNIVERSIDADE DO PORTO

MEB - MESTRADO EM ENGENHARIA BIOMÉDICA 2017/2018

A Dissertação intitulada

"Antibiotic Free Nano/Microparticles to Fight Helicobacter Pylori"

foi aprovada em provas realizadas em 20-09-2018

o júri

Presidente Prof. Doutor Fernando Jorge Mendes Monteiro
Professor Catedrático do Departamento de Engenharia Metalúrgica e de Materiais da FEUP - U.Porto

Doutora Paula Cristina Castro Parreira
Investigadora Pós-Doutoramento do Instituto de Investigação e Inovação em Saúde - i3S - U. Porto

Prof.ª Doutora Liliana do Carmo Santos Grenho
Professora Auxiliar Convidada da Faculdade de Medicina Dentária da U. Porto

O autor declara que a presente dissertação (ou relatório de projeto) é da sua exclusiva autoria e foi escrita sem qualquer apoio externo não explicitamente autorizado. Os resultados, ideias, parágrafos, ou outros extratos tomados de ou inspirados em trabalhos de outros autores, e demais referências bibliográficas usadas, são corretamente citados.

Ana Moura
Autor – Ana Carolina Ferreira Andrade Moura

Faculdade de Engenharia da Universidade do Porto

Abstract

Helicobacter pylori infects more than half of the world's population, and it is responsible for several diseases, namely gastritis and gastric cancer. The recommended treatment consists in a combination of at least two antibiotics and a proton pump inhibitor. However, antibiotic-based therapies had their efficacy rates decreasing over time, mainly due to the growing bacterial resistance to antibiotics. In this context, there is an urge to use antibiotic free alternatives to fight *H. pylori* infection.

Antimicrobial peptides (AMP) are a very promising class of antimicrobial compounds with broad-spectrum of activity (including multidrug resistant microorganisms) and low propensity to induce bacterial resistance. MSI-78A is a derivative peptide from MSI-78, an analogue of the AMP class of magainins, with a reported minimal inhibitory concentration (MIC) of 8 and 16 μg/mL to *H. pylori* ATCC43526 and *H. pylori* ATCC43579, respectively. However, AMP low stability due to protease degradation and aggregation with proteins *in vivo* has limited their clinical applications. One strategy to overcome this problem is their encapsulation or surface immobilization onto bioengineered particles.

During this work, MSI-78A modified with a cysteine extra amino acid on C-terminal (MSI-78A-SH) was immobilized onto chitosan microspheres (ChMic) with a controlled orientation and using polyethylene glycol (PEG) as a spacer (AMP-ChMic). The selected PEG, maleimide polyethylene glycol succinimidyl carboxymethyl ester (NHS-PEG-MAL), has a NHS terminal group, which readily reacts with the free amine groups from the chitosan, and becomes covalently bound to the microsphere. On the other PEG terminal end there is a MAL group, which reacts with the -SH group from the MSI-78A-SH terminal cysteine. ChMic, with sizes ranging from 2 to 7 μm, were produced by spray drying technique using a chitosan solution crosslinked with genipin. PEG and AMP immobilization onto ChMic was evaluated by Fourier transform infrared spectroscopy (FTIR). The amount of AMP immobilized, determined by UV/VIS spectroscopy, was 6.3×10^{-6} μg per AMP-ChMic, translating an estimated reaction yield of 82 %. The microspheres were able to retain their integrity in acidic pH (phosphate buffer pH 2.6), water, phosphate buffered saline (pH 7.4) and ethanol (allowing its sterilization). *In vitro* effect of AMP-ChMic against *H. pylori* was visible within 30 minutes, both in PBS and culture medium, in a concentration dependent way. After 6 h, the highest concentration of AMP-ChMic used, 10^7 ChMic/mL, killed all the bacteria in culture medium.

The results obtained demonstrate that AMP-ChMic have a high potential to become an effective option for *H. pylori* eradication.

Resumo

A bacteria *Helicobacter pylori* (*H. pylori*) infeta mais de metade da população mundial, e é responsável por doenças como a gastrite e o cancro gástrico. O tratamento recomendado consiste na combinação de pelo menos dois antibióticos, com uma bomba inibidora de protões. Estas terapias têm vindo a perder eficácia, especialmente devido ao aumento da resistência bacteriana aos antibióticos. Tendo este problema em conta, surge a necessidade de utilizar alternativas livres de antibióticos para combater a infecção por *H. pylori*.

Os peptidos antimicrobianos (AMP) são uma classe promissora de compostos antimicrobianos com um grande espectro de atividade, que inclui microorganismos multiresistentes, e pouca propensão para induzir resistência bacteriana. O MSI-78A é um peptido derivado do MSI-78, um análogo da classe de AMP das magaininas, e com uma concentração mínima inibitória de 8 µg/mL e 16 µg/mL para *H. pylori* ATCC43526 e *H. pylori* ATCC43579, respetivamente. O uso dos AMP tem sido limitado pela sua susceptibilidade a proteases e agregação com proteínas *in vivo*. Possíveis estratégias para ultrapassar estes problemas passam pela sua encapsulação ou imobilização na superfície de partículas.

Neste trabalho, o MSI-78A modificado com uma císteina no C-terminal (MSI-78A-SH) foi imobilizado em microesferas de quitosano (ChMic) com a orientação controlada, usando um polietileno glicol (PEG) como espaçador (AMP-ChMic). O PEG selecionado, maleimide polyethylene glycol succinimidyl carboxymethyl ester (NHS-PEG-MAL), tem um grupo NHS terminal, que reage com as aminas livres do quitosano e fica covalentemente ligado à microesfera. O outro terminal tem um grupo MAL que reage com o -SH da cisteína terminal do MSI-78A-SH. As ChMic, com tamanhos finais entre os 2 e os 7 µm, foram produzidas pela técnica de spray drying utilizando uma solução de quitosano reticulada com genipina. A imobilização do PEG e do AMP foi avaliada por espectroscopia de infravermelho com transformada de Fourier (FTIR). A reação de imobilização do AMP teve um rendimento de 82 %, com aproximadamente $6.3x10^{-6}$ µg de AMP na superfície de cada AMP-ChMic, determinado por espectroscopia de UV/Vis. As microesferas mantiveram a sua integridade em meio ácido (tampão fosfato pH 2.6), água, tampão fosfato salino (pH 7.4) e etanol (durante a esterilização). O efeito *in vitro* das AMP-ChMic contra a *H. pylori* foi visível nos primeiros 30 minutos, tanto em PBS, com em meio de cultura, sendo este dependente da concentração. Após 6 h, a maior concentração usada, 10^7 ChMic/mL, conseguiu eliminar todas as bactérias em meio de cultura.

Os resultados obtidos demonstram o potencial das AMP-ChMic para se tornarem numa solução viável para a erradicação da *H. pylori*.

Acknowledgements

This thesis would not have been possible without my supervisor, Drª Cristina Martins. I would like to express my gratitude for all the support during this dissertation and for the important conversations throughout the year.

I am extremely grateful to my co-supervisor, Drª Paula Parreira, who has been with me in the lab, since day one and helped me every time. I would like to thank her for the advices and readiness to answer my questions and doubts.

I would also like to thank Drª Catarina Seabra, for always being helpful and for sharing with me precious tips that made my work easier.

I am grateful for the assistance given by the members of my team, BioEngineered Surfaces who always tried to help me when it was necessary and, without any doubt, were essential for the success of my work. Particularly, the assistance provided by Patricia Henriques, regarding the work with the microspheres, and the SEM analysis was greatly appreciated.

I would express my gratitude to Prof. Paula Gomes for the synthesis and characterization of the MSI-78A-SH.

Advice given by Drª Victoria Leiro regarding immobilization conditions was of great appreciation.

I wish to acknowledge the help provided by Drª Berta Estevinho, from LEPABE in the fabrication of microspheres, and size measurements. I would also like acknowledge Dr. Paulo Costa, from FFUP, for allowing me to perform some size measurements.

The help given by André Maia regarding the IN Cell data analysis was highly important for that part of this project.

Then, I would like to thank I3S and INEB for the facilities and all the people working there that always helped me when needed. Specially Ricardo Vidal, María Lázaro and Dalila Pedro for all the help and the readiness to solve all the problems that I faced with the equipment.

Finally, I want to thank all my family, friends, and boyfriend for all the support, and for never letting me go down. You were essential for the success of this stage of my life.

This research work was performed at INEB/i3S (Instituto de Engenharia Biomédica / Instituto de Investigação e Inovação em Saúde) and was financed by FEDER - Fundo Europeu de Desenvolvimento Regional Funds through the COMPETE 2020 -Operational Programme for Competitiveness and Internationalisation (POCI), Portugal 2020. FCT/MCTES through the project PYLORIBINDERS (PTDC/CTM-BIO/ 4043/2014) and NORTE-01-0145-FEDER-000012.

Index

List of figures

List of tables

Abbreviations and symbols

List of abbreviations

AHA	Acetohydroxamic acid
ahx	Aminohexanoic acid
AMP	Antimicrobial peptide
AMP-ChMic	Chitosan microspheres functionalized with PEG and AMP
BabA	Blood group antigen binding Adhesin
BB	Brucella broth
CagA	Cytotoxin-associated immunodominant antigen A
CFU	Colony forming units
ChMic	Chitosan microspheres
ChMic’	Control chitosan microspheres
CLSI	Clinical and laboratory standards institute
DA	Acetylation degree
DHA	Docosahexaenoic acid
EGCG	Epigalllocatechin-3-gallate
FA	Fatty acid
FBS	Fetal bovine serum
FITC	Fluorescein isothiocyanate
FTIR	Fourier transform infrared spectroscopy
h	Hour
H. pylori	*Helicobacter pylori*
IARC	International Agency for Research on Cancer
KBr	Potassium bromide
kDA	Kilodaltons
LEPABE	Laboratório de Engenharia de Processos, Ambiente, Biotecnologia e Energia
LipLLA	Liposomal linolenic acid
LPS	Lipopolysaccharide
MAL	Maleimide

MIC	Minimum Inhibitory Concentration
min	Minutes
MTT	Thiazolyl blue tetrazolium bromide
MW	Molecular weight
NHS	N-Hydroxysuccinimide
NHS-PEG-MAL	Maleimide polyethylene glycol succinimidyl carboxymethyl ester
OD	Optical density
PB	Phosphate buffer
PBS	Phosphate buffered saline
PCR	Polymerase chain reaction
PE	Phosphatidylethanolamine
PEG	Polyethylene glycol
PEG-ChMic	Chitosan microspheres functionalized with PEG
rpm	Rotations per minute
RT	Room temperature
S. mitis	*Streptococcus mitis*
SabA	Sialic acid binding Adhesin
SEM	Scanning electron microscope
SGF	Simulated gastric fluid
TSA	Tryptic soy agar
TSB	Tryptic soy broth
UV/VIS	Ultraviolet/visible spectroscopy
VacA	Vacuolating cytotoxin A
ʎ	Wavelength

Chapter 1

Introduction

Helicobacter pylori (*H. pylori*) is a Gram-negative bacteria responsible for infecting over 80% of the Portuguese adult population [1]. It is associated with several gastric disorders, such as chronic gastritis and peptic ulcer and 1-3% of the chronically infected individuals will develop gastric cancer [2], the 4th most common cancer worldwide that accounted for 754 000 deaths in 2015 [3]. The recommended treatment relies on a combination of antibiotics (usually two) with a proton pump inhibitor [4]. However, the efficacy of these therapeutic schemes have been diminishing all over the world, mainly due to bacterial resistance to available antibiotics, but other factors also account for treatment failure, such as: inadequate length and/or dose of therapy; poor patient compliance and ineffective/difficult antibiotic penetration in the gastric mucosa [1].

As a way of fighting *H. pylori* infection, new solutions are being studied, even though the large majority of the research still focus on more capable alternatives to deliver antibiotics to the infection site, namely by using drug delivery systems. However, the biggest drawback is their poor efficiency against *H. pylori* resistant strains. Antibiotic-free strategies using nanomedicine are scarce, and despite their *in vivo* and *in vitro* good performance, they are failing to reach clinical trials [5]. Among the alternatives with potential to overcome the use of classic antibiotics, antimicrobial peptides (AMPs) present themselves as a promising option. AMPs are known to have a broad spectrum of activity and for being effective in low concentrations without propensity to induce bacterial resistance, since AMPs are thought to selectively damage the bacterial membranes through mechanisms that bacteria find difficult to evade [5,6]. Of the thousands of AMPs identified, only some are reported to have anti- *H. pylori* effect, namely those belonging to the Magainins class. MSI-78A, which is an AMP analogue of MSI-78, commercially known as Pexiganan, is reported to have the best antimicrobial activity against *H. pylori* [8].

This work focuses on the development of a novel bioengineered strategy, allying microparticles and AMP, in order to eradicate *H. pylori*. Microspheres were designed to immobilize an antimicrobial peptide (MSI-78A), previously described as possessing anti- *H. pylori* activity.

The material chosen for the production of the microspheres was chitosan, an extensively used polymer for numerous applications, namely drug delivery systems for gastric settings [9].

To increase the microspheres stability in acidic conditions, the chitosan solution was crosslinked with a nontoxic crosslinker, genipin. The crosslinking forms covalent bonds and prevents chitosan dissolution in low pH. Microspheres were produced by spray drying technique, which yields a large quantity of microspheres in a short time span.

The activity of the AMP functionalized microspheres (AMP-ChMic) was evaluated *in vitro* against the human highly pathogenic *H. pylori* J99 strain.

In summary, the work herein described involved two major objectives:

- Development and characterization of a stable ChMic, functionalized with MSI-78A in a controlled orientation and using a PEG as a spacer, allowing a better AMP exposure from microsphere;

- *In vitro* evaluation of the bactericidal effect of AMP-ChMic against *H. pylori*.

Chapter 2

Helicobacter pylori

2.1 - *H. pylori* overview

In 1984, roughly one century after it was first observed, *Helicobacter pylori* (*H. pylori*) was identified by Robin Warren and Barry Marshall through its isolation from gastric biopsies of patients with gastric inflammation [10]. It was first given the name *Campylobacter pyloridis*, due to its resemblance to the Campylobacter species [11], but it was later found that it possesses several differences, namely fatty acid composition, ultra-structural appearance, and ribosomal RNA sequences [11]. In 1989, it was renamed as *Helicobacter pylori* [12] and in 2005 Warren and Marshal received the Nobel Prize of Medicine for describing the role of *H. pylori* in peptic ulcer disease and chronic gastritis development [13]. Today, *H. pylori* is considered as the etiologic agent of several gastric diseases such as chronic gastritis, gastroduodenal ulcer disease, and gastric cancer [11]. Ultimately, the outcomes of *H. pylori* infection depend on the interactions between pathogen and host, that are dependent of the host genetic susceptibility, environmental influences and strain-specific bacterial constituents [13]. In 1994, it was recognized as a type I carcinogen by the International Agency for Research on Cancer (IARC) Working Group on the Evaluation of Carcinogenic Risks to Humans, including it in the group of agents that are carcinogenic to humans [14]. More recently, the World Health Organization (WHO) listed *H. pylori* among the 16 antibiotic-resistant bacteria that pose the greatest threat to human health [15].

2.2 - *H. pylori* morphology and virulence factors

H. pylori is a microaerophilic Gram-negative bacterium that colonizes the human stomach [16]. It is spiral-shaped but can convert to coccoid-shaped cells in order to overcome hostile environments, such as the presence of antibiotics, nutrient limitation or environmental stress [17]. It is also hypothesized that gastric microbiota contributes to this conversion, through the secretion of diffusible factors, being reported that the gastric bacteria *Streptococcus mitis* (*S. mitis*) has the ability to induce the coccoid conversion [18]. On the other hand, some factors secreted by *H. pylori* promote *S. mitis* survival [18], which highlights the importance of the gastric microbiota relations on the pathogenesis and disease outcome of the infected individuals. *H. pylori* is 2 to 4 µm long and 0.5-1 µm in diameter [17]. It also possesses 4 to 6 unipolar flagella (Fig. 2.1), which confer motility and rapid movements in viscous environments [19], important for the successful gastric colonization [14]. Also, more motile strains have higher infection rates, as highlighted by *in vivo* assays, where the more motile strains were the ones collected from gnobnotic piglets [18,19].

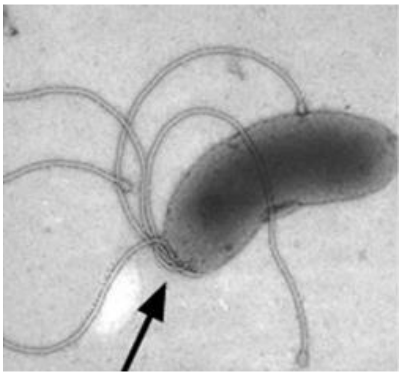

Figure 2.1 - Transmission electron microscopy image of *H. pylori*. Adapted from Douillard *et al.* [22]

H. pylori habitat is the stomach's acidic environment. The stomach presents a pH gradient that can be divided accordingly to its layers: the lumen, with pH 1-2; a mucus layer, and the gastric epithelium with close to neutral pH (pH 5-7) (Fig. 2.2).

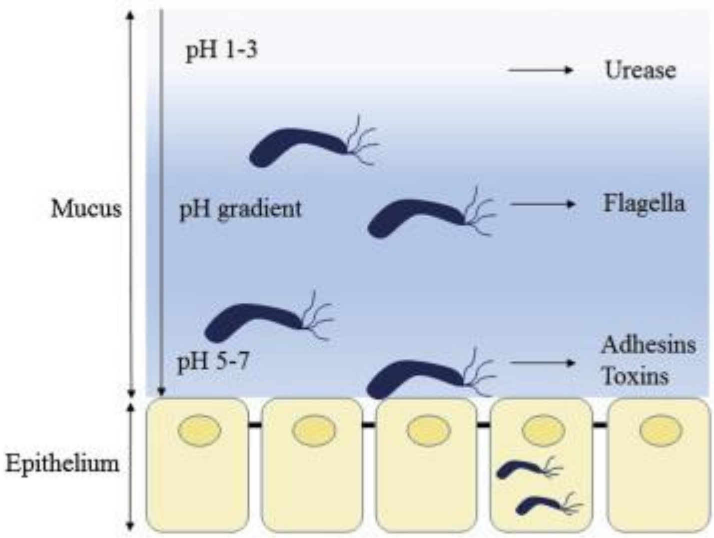

Figure 2.2- Stomach layers schematics and corresponding pH gradient. Adapted from Kao *et al.*[23]

In the lumen *H. pylori* does not have motility [24] and thus it tries to reach the mucosa, where the pH is more neutral. In fact, 80% of the infecting bacteria are found within the gastric mucus [16]. To survive in the low pH of the lumen, bacteria secrete urease, an enzyme that converts urea in ammonia through the reaction represented in eq. 2.1 and eq. 2.2, lowering the acidity of its surroundings, enabling bacteria to thrive in these lumen harsh conditions.
$(NH_2)_2CO$ (aq) + H_2O (l) → CO_2 (g) + $2NH_3$ (aq) (Conversion of urea into ammonia), (eq. 2.1)

NH_3 (aq) + H_2O (l) → NH_4^+ (aq) + OH^- (aq) (Conversion of ammonia into ammonium), (eq. 2.2)

The gastric mucus is normally a gel-like fluid, but as the pH increases, due to the action of urease, it loses some of its elastic properties, which allows *H. pylori* to pass through and reach the gastric epithelium. In addition, *H. pylori* characteristic helical shape allows the penetration in the gastric mucus in a corkscrew-like motion [16].

H. pylori adherence to gastric epithelial cells is essential to establish the chronic infection status. This adherence to the epithelium occurs through bacterial outer membrane proteins, which are able to recognize specific glycan structures expressed by the mucosa. The most studied are the Blood group antigen binding Adhesin (BabA) and the Sialic acid binding Adhesin (SabA). BabA allows the attachment to fucosylated structures, while the SabA is responsible for binding to the sialylated structures present on gastric mucin [24,25]. Another *H. pylori* virulence factor that plays a big role in infection is Vacuolating cytotoxin A (VacA), a protein that induces damage to epithelial cells, by forming vacuoles that increase cytoskeleton changes, transcellular permeability and ultimately lead to apoptosis [27]. The Cytotoxin-associated immunodominant antigene A (CagA) is responsible for codifying a secretion system type IV that is used to translocate bacterial products into the host epithelial cells, leading to the activation of cell-signaling transduction pathways after phosphorilation [27].

The *H. pylori* strains in which CagA is positive and possess a functional BabA and VacA are thought to be more pathogenic and associated with poorer patient prognosis [25]. Although infection would normally trigger host responses, *H. pylori* has the ability to mask its presence by mechanisms of antigenic disguise, in which the bacteria can bind plasminogen and be coated with a host protein, making it practically "invisible" to the immune system. It also possesses a lipopolysaccharide with lower proinflammatory activity than other Gram-negative bacteria, which also allows it to be shielded from the inflammatory and immune system action [28].

Table 2.1 - Most relevant *H. pylori* virulence factors.

Virulence Factors	**Helpful for:**
Urease	Increasing the pH in the surrounding of the bacteria;
Flagella	High motility;
Corkscrew motion	Penetration of mucus;
Adhesins	Adhesion to the mucosa;
CagA	Translocation of bacterial products into epithelial cells;
VacA	Induction of damage to epithelial cells.

2.3 - *H. pylori* prevalence worldwide

Being one of the most successful human pathogens, *H. pylori* infects approximately half of the world's population [29]. As reviewed in Hooi *et al.* [29], the prevalence of *H. pylori* is not uniform around the world, being highly present in Eastern and South-Eastern regions of the Asian continent, as well as in Southern Europe and Latin America (Fig. 2.3) [29]. For most of the African countries, there are no studies performed to access the infected population, leaving a huge gap in the assessment of infection in this continent [29]. Although the rates of infection vary, the higher prevalence is seen in low and middle income countries (developing countries), which are associated with lower life quality and poorer hygiene habits [30]. However, it is noteworthy that inside the same country, large differences in prevalence can be observed, from region to region and also from ethnic minorities to the rest of the population [31]. In the European scenario, Portugal has one of the largest percentages of infection, with above 70% of the population infected [29]. In summary, the high incidence of *H. pylori* worldwide urges the need for effective eradication and treatment methods, as millions of people would benefit from it.

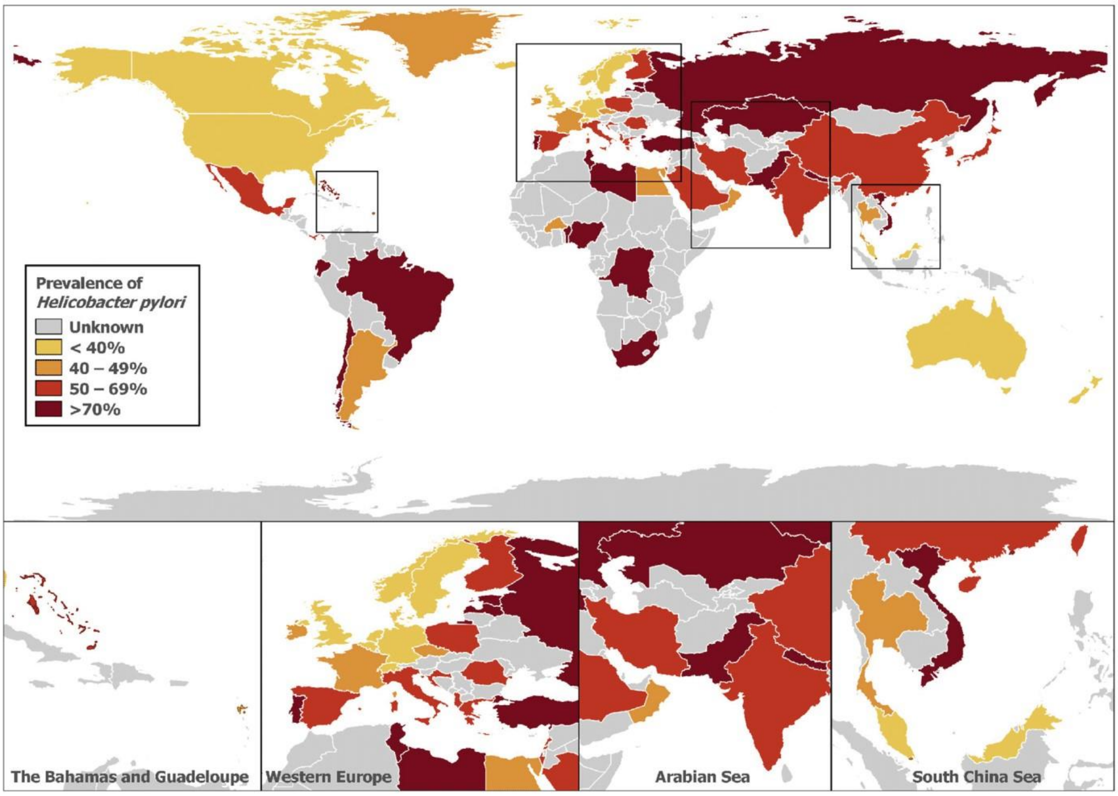

Figure 2.3 - *H. pylori* prevalence worldwide. Data collected from several articles. In Hooi *et al.* [18]

The question of how *H. pylori* became so widespread across the world was raised since it has not been consistently isolated anywhere but in the gastrointestinal tract of humans. The transmission path of the infection is also not clear yet, however human-to-human contact appears to be the most likely form [17], presumably by oro-oral, faeco-oral or gastro-oral transmission routes [32]. The number of *H. pylori* infected individuals is higher in institutionalized patients, as well as in families, when compared to the overall percentages, which only reinforces the thesis of person-to-person transmission [32]. There are also some studies that point as possible ways of transmission contaminated food and water [31].

2.4 - *H. pylori* diagnosis

The Maastricht/Florence Consensus Conference Guidelines stated that the best approach to the diagnostic of *H. pylori* is the urea breath test, as it possesses high sensitivity and specificity [33]. The urea breath test consists in drinking carbon-13 or carbon-14 labeled urea [34]. The urease converts the radiolabeled carbon into carbon dioxide and ammonia and a sample of expired air is analyzed to detect the presence of the radiolabeled carbon [34]. Faeces can also be analyzed to test for the presence of *H. pylori* antigens using specific antibodies [34]. These two methods are non-invasive, whereas a biopsy performed by endoscopy is considered invasive. Nevertheless, an endoscopy allows collecting tissue to perform a polymerase chain reaction (PCR), tissue for histology, rapid urease testing or culturing [35].

2.5 - Available therapies for *H. pylori* treatment

Due to its high incidence worldwide, strategies to eradicate *H. pylori* have been developed. The most commonly accepted treatment is based on a combination of antibiotics, but the regional antibiotic resistance patterns and eradication rates should be taken in consideration when choosing the therapeutic regimen [4,34]. As a first line of therapy, there are different treatments regimens, such as the triple therapy, bismuth-containing quadruple therapy, non-bismuth-containing quadruple regimen, sequential therapy, concomitant therapy, and hybrid therapy (Fig. 2.4) [37]. All can be adapted to the patient individual characteristics, both in length and/or by changing the antibiotics and its daily dosages. The triple therapy is the most common, with duration of 7 to 14 days, and involves the usage of a proton pump inhibitor conjugated with two antibiotics, clarithromycin and amoxicillin or metronidazole, twice a day. Sequential therapy uses an innovative administration strategy, since it begins for five days with a proton pump inhibitor and amoxicillin followed by another five-day period with proton pump inhibitor, clarithromycin and nitroimidazole [37]. However, the success rates of this combined antibiotic regimens are decreasing to values considered unacceptable by The European Helicobacter Study Group, as stated in the Maastricht V/Florence Consensus (<80% of eradication) [4,34].

Treatment failure is associated with several factors, namely:

(1) the increasing rate of antibiotic resistant bacteria (Fig. 2.5), concerning both primary and acquired resistance. Also, infection by multiple strains is common, leading to survival of the resistant strains, enabling the spreading of genes encoding information for drug resistance. Also, the selective pressure derived from the wrongful use of antibiotics plays a major part in the resistance to antibiotics issue [38];

(2) the gastrointestinal tract has a broad pH range that varies accordingly to the presence/absence of food, and in which not all of the antibiotics are active [7,37];

(3) the oral route is the most common for antibiotic administration, but it limits drug bioavailability, since the layer of gastric mucous behaves as a barrier, hindering the antibiotic to reach the epithelial cells, where *H. pylori* is attached [40];

(4) the patients' lack of commitment to the selected therapy, because of the various side-effects and the complex dose regimens [38];

(5) the lifestyle adopted by the patient also impacts the success, since coffee intake and smoking are related with treatment failure [7].

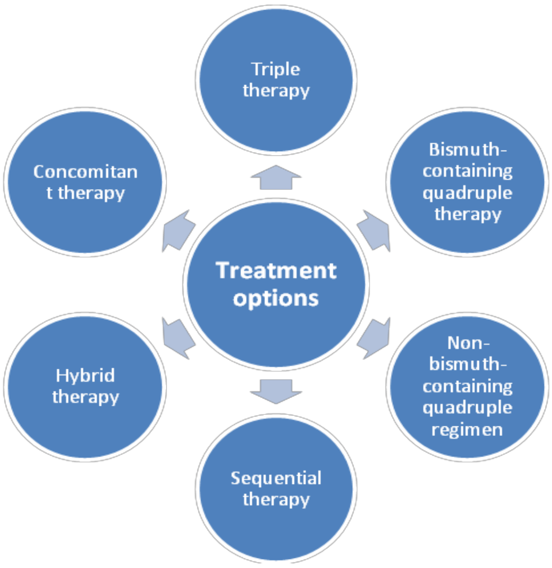

Figure 2.4 - Summary of antibiotic therapies available for *H. pylori* eradication.

Clarithromycin is a potent antibiotic used for several therapeutic purposes, being also one of the antibiotics to which *H. pylori* has great resistance rates, ranging from 5.46% to 30.8% [41]. One possible explanation for these numbers is the common use of clarithromycin to treat respiratory infections [42].

Metronidazole is the major responsible for treatment failure when it is one of the components of the therapeutic scheme, as it is the one that presents the higher resistance rates, reaching an average of approximately 80% in the African countries [41]. It is commonly used to substitute amoxicillin in patients allergic to penicillin, namely in treatment of dental, gynecological and parasitic related infectious diseases [41], which can impact the high resistance observed [43].

Amoxicillin is one of the antibiotics with less resistance associated to it [41]. Europe and North America have low rates of resistance, close to zero, in contrast with Africa and Asia, where amoxicillin can be bought without a medical prescription, leading to its misuse and consequent resistance acquisition [41].

Tetracycline is a bacteriostatic and broad spectrum agent, active against *H. pylori* [41]. It is also commonly used to treat other infectious diseases, however its resistance is still low in the majority of the world [41].

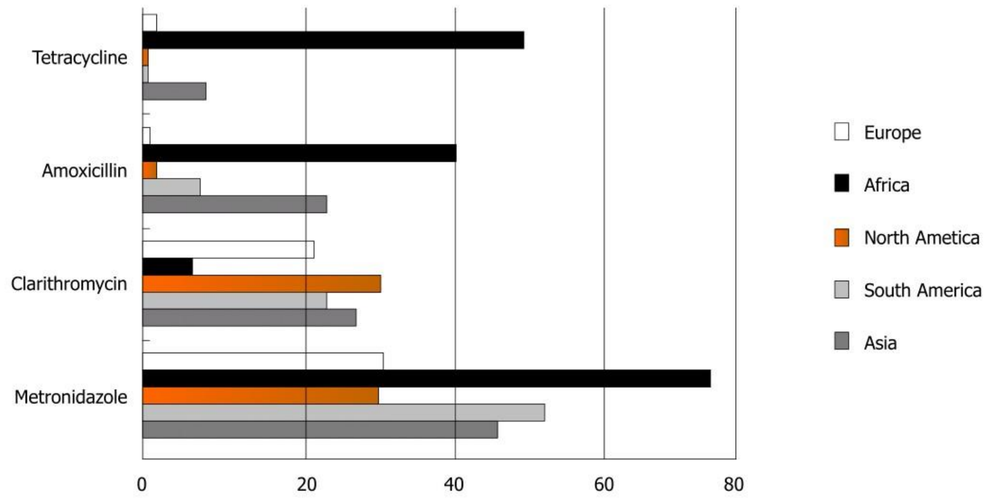

Figure 2.5 - Antibiotic resistance prevalence. The rate of resistance of the four most used antibiotics in Europe, Africa, North America, South America and Asia in the past 6 years. In Ghotaslou *et al.* [30]

Currently, treatment consists in the oral administration of antibiotics, with the already mentioned drawbacks. In order to extend the residence time of the drugs in the stomach, and to potentiate its effects, several alternatives are appearing. A common way to achieve this goal is to design drug delivery systems, where the antibiotic can be encapsulated, aiming to improve the efficacy of the treatment by preventing drug degradation in the stomach acidic pH, and thus, allowing it to have a stronger/more direct effect [9]. Several types of particles have been developed, based on different properties, against *H. pylori* [7,41,42]. These bioengineered particles have demonstrated good *in vitro* and *in vivo* results, when compared to standard therapies, or the free antibiotic, although no clinical trials were yet performed to assess their performance on Humans. One of the disadvantages of these drug delivery systems is that they still rely on antibiotics to eradicate the bacteria, making them not suitable for cases of patients with antibiotic resistance, who require other treatment approaches, preferentially antibiotic-free alternatives. However, and despite the above-mentioned drawbacks, the majority of the research lines undergoing to date are still focused on antibiotic-based strategies.

Chapter 3

Antibiotic-free alternatives

3.1 - Alternative options

There is an urgent need for the development of novel alternatives to fight *H. pylori*, since bacterial resistance rates to antibiotics continue to reach worryingly levels across the globe.

3.1.1 Vaccines

One of the alternatives under study is the development of a prophylactic and/or a therapeutic vaccine [46]. A therapeutic vaccine would not only clear the organism from *H. pylori*, but also protect it against reinfection [47]. One of the winning argument for this approach states that it is virtually impossible to screen all the infected people, as it will most likely lead to prohibitive costs of antimicrobial treatment. Therefore, a vaccine would be the best option, since it can be administered in early life and act as a preventive measure [48]. There are four requirements for an optimized efficient vaccine: an optimal dose and frequency of administration, an adequate antigen, a strong immunogenicity accomplished by the inclusion of a carrier or an adjuvant, and a suitable antigen [48]. The *in vivo* results obtained are good, especially those when the subjects tested were neonatal mice, which can indicate that the vaccine should be taken in early stages of life [48]. To this date, 9 clinical trials were carried out [46–54]. All of them were considered unsuccessful, due to the lack of induced immunity protection, except one, containing ureaseß protein subunits, which claims to have a 72% of efficacy [57]. The failure of the vaccines can be attributed to *H. pylori* ability to evade the immune response which is facilitated by its virulence factors [58].

3.1.2 Probiotics

Probiotics are *"live microorganisms that, when administered in adequate amounts, confer a health benefit on the host"* as defined by the Food and Agriculture Organization and the World Health Organization [59]. These microorganisms have demonstrated activity against *H. pylori*, and are a large-scale, low-cost alternative [60]. Among the more common probiotics are *Lactobacillus* spp., *Bifidobacterium* spp., and *Streptococcus* spp. [61]. Some probiotics are able to produce antimicrobial compounds that inhibit potential pathogens, namely the *Lactobacillus acidophilus* CRL 639, that secretes an antibacterial substance with anti- *H. pylori* activity [62]. *H. pylori* crucial adhesion to the gastric mucosa can also be inhibited when there is a large number of probiotics covering non-specifically the receptor sites or competing for the specific receptors [63]. A few clinical trials have been conducted attempting to see the effect of the probiotics alone or as adjuvants, *i.*e, combined with other therapies, as well as what strains were more effective against *H. pylori* [61]. However, most of these studies proved this approach to be ineffective in successfully eradicating *H. pylori* [57,59].

3.1.3 Phytotherapy

Plants have been used for centuries to cure illnesses. The majority of the available studies describe efficacy of phytotherapies *in vitro*, with just a few cases reporting effective bacterial eradication in *in vivo* or in clinical trials settings [64]. One of the possible explanations for this failure is the compounds inability to reach the bacteria, due to the acidic conditions of the stomach [64]. In 2014, Wang *et al.* [65] reviewed the plants extracts already studied against *H. pylori* and came across the following results: only 2.9% (1/34) of the extracts exhibited a strong activity (Minimum Inhibitory Concentration (MIC) < 10 µg/mL) and most studies, 82.4% (28/34), revealed weak to moderate or weak activity, The best result reported belongs to the *Impatiens balsamina* L. (Balsaminaceae), and its MIC is compared to that of amoxicillin, one of the strongest antibiotics available [66]. On the other hand, plant compounds presented better results regarding their activity, when compared with the extracts, more than 50% were considered strong, by the above-mentioned MIC criterion. [2-methoxy-1,4-naphthoquinone] [67], terpinen-4-ol [68], pyrolidine [68], 1-methyl-2-[(Z)-8-tridecenyl]-4-(1H)-quinolone [69] , and 1-methyl-2-[(Z)-7-tridecenyl]-4-(1H)-quinolone [69], stood out as having a MIC lower than 1 µg/mL [65]. Plants exhibit different action mechanisms against *H. pylori*, such as anti-adhesion activity, urease activity inhibition and oxidative stress [65]. The natural constituents of plants are able to ameliorate patients' health, however they cannot be seen as a solo treatment [70].

3.1.4 Antimicrobial Peptides

Antimicrobial peptides (AMP) are simple, natural occurring peptides with antimicrobial properties. They are small, 1 to 5 kDa, 10 to 25 amino acids and most of them are cationic [71]. AMPs have tendency to form amphipathic structures in non-polar solvents. They can function as potent, broad-spectrum antibiotic with a rapid killing effect, having fungicidal, bactericidal, tumoricidal and viricidal properties. One of the most interesting AMP characteristics is their low tendency to promote bacterial resistance. It happens because AMP selectively damage the membrane, in a way which the bacteria has trouble to escape, and while this theory is not proved, it is the most widely accepted [6,7]. AMP structure is easily modified, which also contributes to making their surface immobilization easy [72]. Some of the AMPs reported to efficiently eradicate *H. pylori* are represented in the Table 3.1, along with their MIC and the *H. pylori* strain against they were tested. Among them, is the MSI-78, commercially known as Pexiganan, that belongs to the magainin family, a class of natural peptides isolated from amphibian skins [7] and MSI-78A, a derivative of MSI-78, with a difference in one amino acid. MSI-78A proved to have a stronger effect against *H. pylori* than MSI-78. The cathelicidins are another family of antimicrobial peptides with proven effect, namely protecting against *H. pylori* colonization [70,71].

Table 3.1 – AMP effective against *H. pylori*.

Antimicrobial Peptide	Amino acid sequence	MIC	*H. pylori* strain	Reference
SolyC	FSGGNCRGFRRRCFCTK-NH_2	10-15 μg/mL	Bacterial isolates from hospitalized patients	[75]
MSI-78	GIGKFLKKAKKFGKAFVKILKK	2 μg/mL	43504	[76]
		64 μg/mL	43526	[8]
		64 μg/mL	43579	
MSI-78A	GIGKFLKKAKKFAKAFVKILKK	8 μg/mL	43526	[8]
		16 μg/mL	43579	
Odorranain-HP	GLLRASSVWGRKYYVDLAGCAKA	20 μg/mL	NCTC11637	[77]
$C_{12}K$-$2B_{12}$	C12K-KlK-KlK	9 μg/mL	G27	[78]
		11 μg/mL	7.13	
		14 μg/mL	J99	
		14 μg/mL	HPAG1	
		32 μg/mL	SS1	
		32 μg/mL	26695	
TP4	FIHHIIGGLFSAGKAIHRLIRRRRR	3 μg/mL	43504	[79]
		3 μg/mL	700392	
		3 μg/mL	43629	
		3 μg/mL	CIHC-028	
Epi-1	GFIFHIIKGLFHAGKMIHGLV	8-12 μg/mL	43504	[80]
		8-12 μg/mL	700392	
		8-12 μg/mL	43629	
		8-12 μg/mL	CI-HP028	
Pardaxin	GFFALIPKIISSPLFKTLLSAVGSALSSSGGQE	>25 μg/mL	43504	
		>25 μg/mL	700392	
		>25 μg/mL	43629	
		>25 μg/mL	CI-HP028	
Pleurain-A1	SIITMTKEAKLPQLWKQIACRLYNTC	30 μg/mL	NCTC11637	[81]
Pleurain-A2	SIITMTKEAKLPQSWKQIACRLYNTC	30 μg/mL	NCTC11637	

3.2 - Novel antibiotic-free bioengineered strategies

Few studies were made envisioning alternatives that do not involve the use of antibiotics. In the next section, some of them are described. The subsection division was based on the type of material from which the studied alternative derives.

3.2.1 Chitosan based

Chitosan is obtained from chitin (Fig. 3.1), a polysaccharide that is the major component of the crustaceans shells [82]. It presents several interesting properties that allows it to be used in several research areas, such as the pharmaceutical and biomedical [83,84]. In order to obtain chitosan, chitin undergoes a process of N-deacetylation, being the degree of acetylation (DA) based on the percentage of acetyl groups present in the chitosan molecule [85]. It is generally insoluble in aqueous solutions above pH 7, but readily dissolves in acidic conditions, due to protonation of the free amino groups [86]. Chitosan is very versatile, being often conjugated with several molecules, and the amino and hydroxyl groups are responsible for the easiness in chemically modifying its structure. Moreover, chitosan is known to be biocompatible, biodegradable, biologically inert, safe for human use and in the natural environment [83,84]. It also presents mucoadhesive properties [85], as a consequence of the electrostatic interactions established between the negative charged gastric mucins, at the stomach pH, and the positive charged amino groups [88]. Chitosan has also been reported as having a broad-spectrum of antimicrobial effect, namely against fungi and bacteria [89].

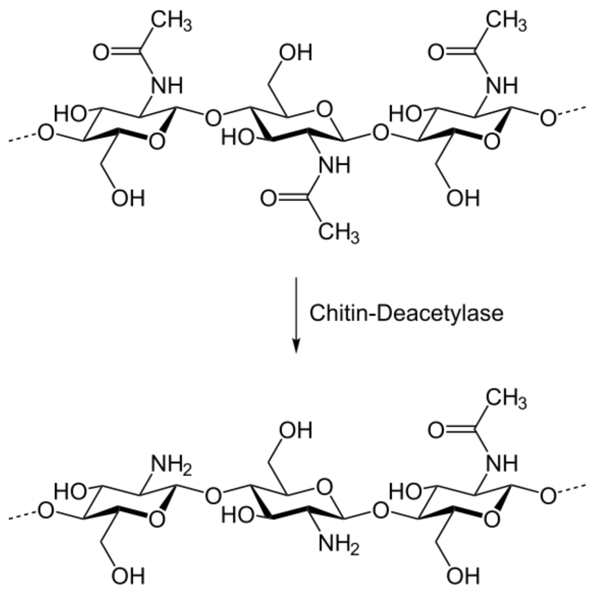

Figure 3.1 - Chitin to chitosan reaction.

One of the first studies using chitosan nanoparticles against *H. pylori* was conducted in 2009 by Luo *et al.* [90]. The used nanoparticles were obtained by the polymeric dispersion method. This study concluded that the bacteriostatic effect, i.e ability to unable growth, of the chitosan nanoparticles was better at lower pH, with an optimal value around pH 4, and that the higher the deacetylation degree, the better the antimicrobial properties [90].

In the same year, Lin *et al.* assessed the effect of chitosan/heparin nanoparticles on simulated gastric fluid [91]. Heparin is reported to boost the healing rate of a gastric ulcer, associated with the regeneration of the mucosa, proliferation, and angiogenesis [92]. It was reported that pH responsive chitosan nanoparticles are stable at pH 1.2–2.5 and can posteriorly prevent drug inactivation by gastric acid [91]. The nanoparticles were able to interact with *H. pylori* infection sites by infiltrating trough cell-cell junctions where, at pH 7, they disintegrated [91].

As previously mentioned, chitosan is soluble in acidic conditions, which limits its use for gastric settings. Therefore, enhancing the chemical stability and mechanical strength of chitosan by crosslinking is a very common approach [86]. Genipin is a non-toxic crosslinker that binds covalently to two chitosan primary amines, leading to the formation of a heterocyclic amino linkage and a secondary amide (Fig. 3.2) [93]. The amount of primary amines left available in the chitosan chain influence its mucoadhesive properties and, therefore, the crosslinking process must be carefully controlled [94].

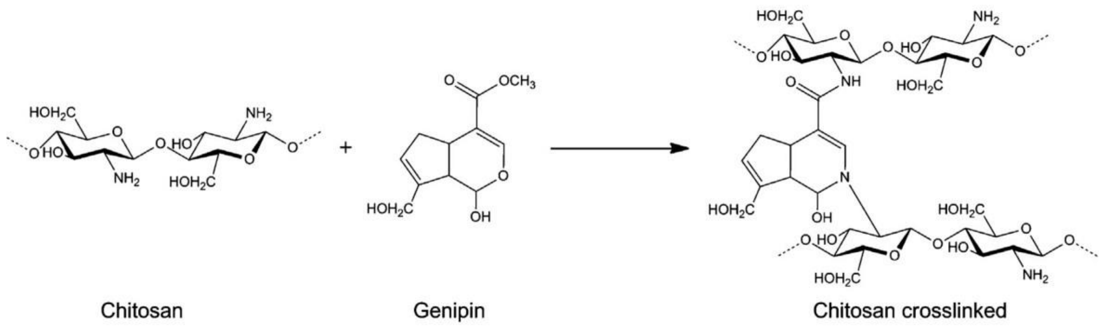

Figure 3.2 - Crosslinking reaction between chitosan and genipin. In Fernandes *et al.* [94]

Chitosan microspheres crosslinked with genipin were designed with the intention of acting as "*H. pylori* binders" by Fernandes *et al.* [94]. It was described that the crosslinking level influenced the size, charge and stability in acid conditions, as well as the capacity to absorb soluble mucins [94]. Gonçalves *et al.* [95] demonstrated that these microspheres (with diameter ~ 170 µm) are non-cytotoxic and able to remove bacteria adhered to gastric cells, as well as preventing its adhesion. Using these same microspheres, Gonçalves *et al.* created a decoy by immobilizing Lewis b glycans on the microspheres surface, which led *H. pylori* BabA adhesin to attract and specifically bind to them [96]. Nevertheless, the downside of this strategy is its strain specific nature, since it can only be used with BabA+ strains.

In 2014, Lin *et al.* assessed the efficiency of fucose-chitosan/gelatine/epigallocatechin-3-gallate (EGCG) nanoparticles *in vivo* [97]. This strategy was based on a dual approach: in one hand, EGCG is an ingredient of green tea known to have anti-*H. pylori* activity, namely targeting urease [95,96]; on the other hand, *H. pylori* is able to specifically bind to specific carbohydrate compounds, such as fucose [100], which increased the affinity of the bacteria towards the designed nanoparticles. These nanoparticles were successful in inhibiting bacterial growth, while also reducing the associated gastric inflammation [97]. The conjugation fucose-chitosan was used again with a heparin shell to study the controlled release of berberine [100]. Berberine is an alkaloid, derived from a plant of the barberry species, the *Coptis chinensis*, and it has antihypertensive, antibacterial, antiprotozoal, anticholinergic and anti-inflammatory properties [100]. These heparin shelled nanoparticles were able to protect berberine in the gastric settings, enhancing its effect and ultimately allowing it to be active against *H. pylori* [100]. Another study using a heparin shell was performed in 2011 using chitosan nanoparticles loaded with berberine [101]. These nanoparticles were more successful in inhibiting bacterial growth in comparison with the berberine alone in solution and were also efficient in decreasing the cytotoxic effects of berberine [101].

In 2015, Zhang *et al.* tested *in vivo* the efficacy of chitosan-alginate nanoparticles for Pexiganan delivery. They were able to adhere to gastric mucosa and stay for prolonged time periods, proving to be more efficient in *H. pylori* clearance than the Pexiganan suspension alone [102].

Table 3.2 - Developed chitosan based particles.

Type of particle	**Mode of action**	**Production method**	**Main conclusions**	**Reference**
Chitosan nanoparticles	*H. pylori* binding	Polymeric dispersion	Better bacteriostatic effect at pH 4	[90]
Chitosan/heparin nanoparticles	Drug Delivery	Ionic gelation	Prevented drug degradation and interacted with *H. pylori* infection sites	[91]
Chitosan/genipin microspheres	*H. pylori* binding	Ionic gelation	Non-cytotoxic *in vitro*, removed and prevented bacterial adhesion	[94], [95]
ChMic modified with glycans	*H. pylori* binding	Ionic gelation	Removed and prevented adhesion of *H. pylori* BabA positive strain	[96]
Fucose-chitosan/gelatin/EGCG nanoparticles	Drug Delivery - EGCG	Ionic gelation	Inhibited *H. pylori* growth and reduced inflammation	[97]
Fucose-chitosan/heparin nanoparticles	Drug Delivery - Berberine	Ionic gelation	Prevented drug degradation, had a clearence effect and reduced inflammation	[100]
Heparin/chitosan nanoparticles	Drug Delivery - Berberine	Ionic gelation	Prevented drug degradation, i *H. pylori* growth inhibition and decreased berberine	[101]
Chitosan-alginate nanoparticles	Drug Delivery - Pexiganan	Ionic gelation	Adhered to gastric mucosa and had better eradication results than Pexiganan in suspension	[102]

3.2.2 Lipid based

In 2003, Umamaheshwari *et al.* developed a nanoparticle able to locate and anchor a drug delivery system, by designing lectin-conjugated gliadin nanoparticles [103]. This formulation took advantage of the fact that gliadin is a protein with a strong adhesive capacity towards the gastrointestinal mucosa, due to its lipophilic and neutral residues [103]. Lipophilic components interact with the biologic tissue via hydrophobic interactions, whereas hydrogen-bonding interactions are promoted by neutral amino acids [103]. Lectins are a group of carbohydrate-binding proteins, some of them known to have receptors on *H. pylori* surface, such as fucose and mannose-specific lectins [104]. The results obtained proved the efficacy of the nanoparticles that were able to completely inhibit *H. pylori* growth *in vitro* within 12 h [103].

A different approach was taken by the development of a lipobead, envisioning blockage of *H. pylori*'s adhesion to gastric cell, therefore inhibiting infection. The lipobead consisted in a polyvinyl alcohol xerogel bead containing acetohydroxamic acid (AHA), surrounded by phosphatidylethanolamine (PE) [105]. PE is a lipid present in the human stomach that also accounts for *H. pylori* adhesion [106], while AHA is a small molecule able to permeate bacterial cells and inhibit *H. pylori*'s urease activity [105]. The lipobeads had successful results in protecting AHA from gastric settings, as well as inhibiting bacterial growth *in vitro* [105].

One of the most studied lipid-based strategies are liposomes, which are spherical vesicles composed of a phospholipid bilayer. Liposomes can act as delivery systems, especially since they easily fuse with bacterial membrane [107]. At the same time, fatty acids (FA) have gained renewed attention after their antibacterial activities against several bacteria, namely against *H. pylori*, were demonstrated [107].

The first study using a antibiotic-free liposomal formulation was performed in 2012 by Obonyo *et al.* [108], using a liposome loaded with linolenic acid (C18:3) (LipoLLA). This novel formulation exhibited bactericidal activity, effectively killing *H. pylori* spiral and coccoid forms [108]. It was also demonstrated that bacteria did not develop resistance to LipoLLA, as it occurred when free LLA was administered [108]. The *in vivo* results of the LipoLLA revealed excellent biocompatibility to healthy mouse stomach and ability to fuse with the bacterial membrane, thus releasing the LLA. As it effectively reduced the bacterial load, it also reduced *H. pylori* induced proinflammatory cytokines [109]. To further evaluate the LipoLLA potential, its effect was compared to liposomal stearic acid (C18:0) and to oleic acid (C18:1). LipoLLA had the biggest bactericidal effect, completely killing the bacteria after 5 minutes. This study also unraveled LipoLLA mechanism of action, as it leads to cytoplasmic content leakage by affecting the membrane integrity through structural changes [110].

Besides the liposomes, there are other encapsulation strategies for fatty acids. Nanostructured lipid carriers are an alternative, as they can be used to encapsulate poor water-soluble drugs. In 2017, docosahexaenoic acid (DHA) was successfully encapsulated into a nanostructured lipid carrier and this formulation enhanced DHA bactericidal effect *in vitro* [111].

Table 3.3 - Developed lipid based particles.

Type of particle	Mode of action	Production method	Main conclusions	Reference
Lectin conjugated Gliadin nanoparticles with AHA	Drug Delivery - AHA	Desolvation	Inhibited *H. pylori* growth *in vivo*	[103]
PE liposomes anchored polyvinyl alcohol xerogel beads bearing AHA	Drug Delivery - AHA	Lipid cast film hydration	Protected the drug and inhibited bacterial growth	[105]
Liposomal linolenic acid	Drug Delivery – Linolenic acid	Vesicle extrusion	Killed the bacteria and reduced the inflammation	[108]–[110]
DHA-loaded nanostructured lipid carriers	Drug Delivery - DHA	Hot homogenization	Bactericidal and non-cytotoxic	[111]

3.2.3 Metallic based

Silver has been used for centuries for several medicinal purposes, from wound healing to bone regeneration and gastrointestinal diseases [112]. Regarding gastric application, silver is considered as an antiulcer agent, being this reason why studies found with metal compounds all have silver in common.

In 2012, Amin *et al*. synthesized silver nanoparticles, and characterized their anti- *H. pylori* activity using the agar dilution method [113]. Their effect was compared to standard drugs, and it was demonstrated that the MIC for silver nanoparticles was 2-8 μg/mL, exhibiting better performance than silver nitrate, tetracycline and metronidazole, but nonetheless less potent when compared to amoxicillin (0.125-4 μg/mL) and clarithromycin (0.125-8 μg/mL) [113]. Inhibitory activity against urease was also reported [113]. A couple of years later, a new study was performed assessing the therapeutic effects of silver nanoparticles *in vivo*, using male albino Wistar rats, and their bactericidal activity was confirmed [114].

Although few studies regarding the use of metallic non-antibiotic alternatives are available, other metals are beginning to be explored for use in gastric settings. For instance, a zinc(II)–famotidine complex [115] was tested against *H. pylori*.

Table 3.4 - Developed metallic based particles.

Type of particle	Mode of action	Production method	Main conclusions	Reference
Silver nanoparticles	Contact	Green chemistry	Bactericidal effect	[113], [114]

3.2.4 'Others' based

Garcinia mangostana extract was encapsulated in ethyl cellulose methyl cellulose nanoparticles to assess their *in vivo* effect. These nanoparticles were able to adhere to the stomach mucosa and reduce bacterial adhesion, which was not observed with the non-encapsulated form [116].

A novel three-layer structure was studied to enhance drug concentration and retention time [117]. The first layer was composed of berberine hydrochloride encapsulated in Eudragit® cores, for the control of berberine release. Then, the cores were surrounded by a mucoadhesive layer of thiolated chitosan, which was coated with hydroxypropyl methylcellulose acetate maleate that degrades below pH 3.0 [117]. *In vivo*, results demonstrated that this novel structure can function efficiently as a drug delivery system for berberine [117].

In 2015, Khalil *et al*. [118] pursued a different approach by encapsulating lactic acid bacteria (*Lactobacillus plantarum*, *Lactobacillus acidophilus*, and *Lactobacillus bulgaricus* DSMZ 20080) in a chitosan alginate capsule. This strategy demonstrated the ability to successfully down regulate *H. pylori* infection in mice. In a similar attempt, Fulgione *et al*. [119] combined lactoferrin with cell free supernatant from the probiotic *Lactobacillus paracasei* entrapped in biomimetic hydroxyapatite nanoparticles. These nanoparticles had better results when compared with the conventional therapy, as they proved to induce immune response and demonstrated anti-inflammatory activity [119].

Table 3.5 - Developed 'others' based particles.

Type of particle	Mode of action	Production method	Main conclusions	Reference
Garcinia mangostana extract - loaded ECMC nanoparticles	Drug delivery – Garcinia mangostana extract	Spray drying	Prevented drug degradation and *H. pylori* adhesion	[116]
Three layers Eudragit structure	Drug delivery - Berberine	Emulsification /coagulation coating	Prevented drug degradation; mucoadhesive	[117]
Microencapsulation of acid lactic bacteria	Probiotic delivery	Emulsion	Inhibited bacterial growth	[118]
Lactoferrin delivered by nanoparticles of hydroxyapatite	Probiotic delivery	Precipitation	Antibacterial and anti-inflammatory effect	[119]

3.3 - Objective

The main objective of this work was to develop a novel non-antibiotic based bioengineered strategy to eradicate *H. pylori*. The herein proposed strategy relies on the use of the previously mentioned MSI-78A antimicrobial peptide covalently immobilized on the surface of a ChMic - AMP-ChMic (Fig. 3.3). To achieve this goal, custom-made microspheres were produced by spray drying, using chitosan crosslinked with genipin. The immobilization of the selected AMP in a controlled manner, attempts to overcome the major drawbacks associated to their *in vivo* performance, while also promoting AMP exposure and interaction with *H. pylori*, enabling bacterial consequent killing. These AMP-ChMic intend to demonstrate their efficacy against *H. pylori* as an antibiotic-free bioengineered strategy.

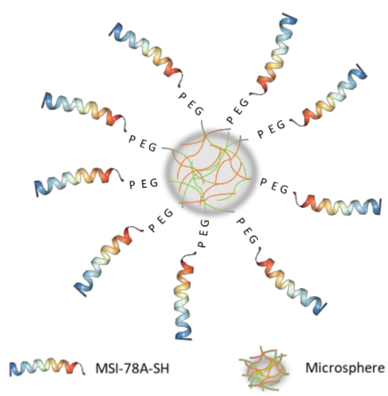

Figure 3.3 - Schematic representation of AMP-ChMic.

Chapter 4

Materials and Methods

4.1 - Chitosan Purification

Chitosan purification was performed by the re-precipitation method [120]. Briefly, commercial squid pen chitosan (with degree of acetylation (DA) of 6 % and 16 %; France Chitine) was dried at 60 °C, in a vacuum oven, during 24 h. Afterwards, chitosan was hydrated with type II water (1 g per 198 mL) under slow magnetic stirring, at 4 °C for 24 h and protected from light. Chitosan dissolution was achieved by adding 2 mL of glacial acetic acid (AppliChem Panreac, US) to the previously mentioned solution, under stirring and at RT, followed by a 20 µm filtration (Merck Millipore, United States) to remove non-dissolved chitosan particles. This filtered solution was precipitated by neutralization with the dropwise addition of 1.0 M sodium hydroxide (Merck, Germany) and under strong magnetic stirring, until pH 12 was reached (pH indicator strips; VWR Chemicals, United States). Then, chitosan was rinsed with type II water by centrifugation at 3000 *g* (Eppendorf® 5810R, Germany), until pH 7 was reached (pH indicator strips; VWR Chemicals, United States). Lastly, chitosan was freeze dried (Freezone 2.5 Plus; Labconco, Germany) for 72 h and posteriorly grinded (A10; Ika, Germany) in order to obtain a fine powder. The DA was determined by FTIR (Perkin-Elmer, United States).

4.2 - Chitosan Microspheres (ChMic) Production

4.2.1 Crosslinking Reaction

The purified chitosan powder (obtained as mentioned in 4.1) was hydrated and then dissolved following the previously described protocol, in order to obtain a purified chitosan solution (0.46 % (w/v)). Then, the solution was incubated with genipin (Wako Chemicals, United States), the selected crosslinking agent. To optimize crosslinking process, several parameters were evaluated according to Table 4.1. All the assays were performed using an orbital shaker at 150 rpm (IKA KS 3000, Germany) and using chitosan with 16 % DA (for comparison with previous results obtained by our group).

Table 4.1 - Crosslinking conditions tested.

Sample	Genipin (mM)	Temperature (°C)	Duration (h)
A	2.5	37	2
B	2.5	50	2
C	1.0	50	24
D	0.5	50	24
E	0.25	50	24

Color change was evaluated for all the samples and their viscosity evaluated through rheometry (Kinexus, Malvern, United Kingdom). The selected conditions for microspheres production were: chitosan solution (with DA 6 and 16 %) at 0.46 % (w/v), 2.5 mM of genipin 2 h incubation at 37 °C (Fig. 4.4).

4.2.2 Spray Dryer

Microspheres were produced using the spray drying technique [121] in a BÜCHI B-290 advanced with a standard 0.5 mm nozzle spray dryer (Flawil, Switzerland) at LEPABE, UPorto. The settings for microspheres production were the following: 4 mL/min (15 %) for solution flow rate, 40 m^3/h of air flow rate, air pressure of 6.5 bar and inlet temperature and outlet temperature of 120 °C and 66 °C, respectively (Fig. 4.4). ChMic were stored at RT, protected from light in a desiccator until further use.

4.3 - AMP Immobilization

AMP immobilization onto ChMic was performed in a sequential two-step reaction (Fig. 4.1):

4.3.1) Immobilization of a PEG spacer onto ChMic, to improve AMP exposure from the surface plus introduction of specific functional groups for AMP controlled immobilization and orientation (PEG-ChMic);

4.3.2) AMP immobilization through thiol-MAL chemistry, in order to control surface orientation of the AMP (AMP-ChMic).

The selected microspheres were prepared using chitosan with 6 % DA (ChMic_6) (Fig. 4.4), due to their higher number of free amines present in the polymer, which is important for both AMP immobilization as well as to retain microspheres mucoadhesiveness.

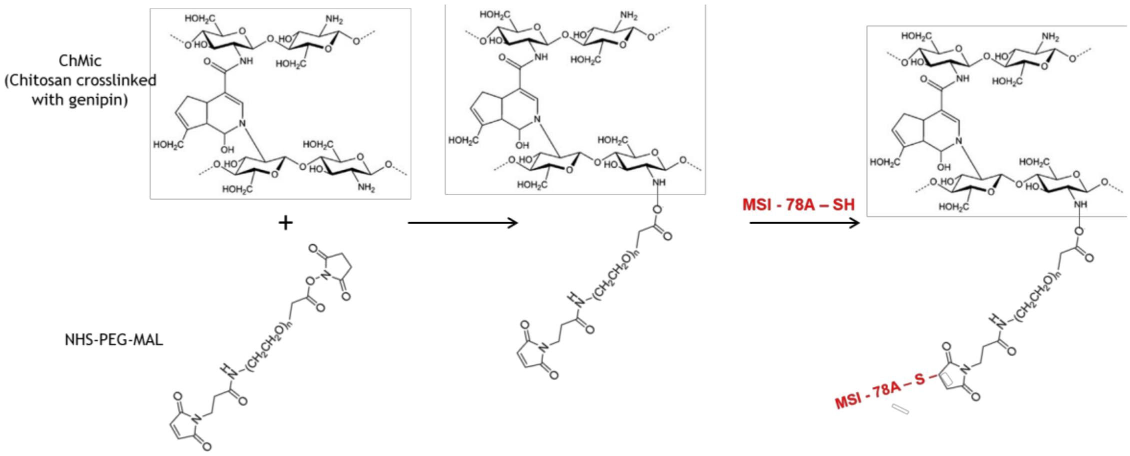

Figure 4.1 – MSI-78A-SH immobilization mechanism on ChMic.

4.3.1 PEG Immobilization on ChMic (PEG-ChMic)

Dry ChMic_6 were suspended in PB (pH 6.6) in a 1 mg/mL concentration and placed under the ultrasound probe VibraCell™ (Sonics & Materials, United Kingdom) for 5 min, amplitude 70 %, to minimize particles aggregation.

Then, a heterobifunctional PEG (NHS-PEG-MAL; maleimide polyethylene glycol succinimidyl carboxymethyl ester; MW 5000 kDa; Jenkem, United States) was added to the microspheres solution (1:2 ratio; w/w). To optimize the linkage between the chitosan free amines (-NH_2) and the PEG NHS group, NHS-PEG-MAL was added to the microspheres solution at different time points: 0 h, 2 h and 4 h. NHS-PEG-MAL was incubated for a total 10 h after the first addition, at RT and in an orbital shaker at 150 rpm (IKA KS 3000, Gemany). To remove any non-immobilized PEG, the solution was placed in a dialysis bag with a 10 kDa cut-off (Spectrum Labs, US) during 16 h at RT with mild stirring. After, PEG-ChMics were centrifuged at 10 000 *g*, resuspended in 1.5 mL of PB (pH 6.6), and ultrasonicated as previously mentioned.

4.3.2 AMP Immobilization on PEG-ChMic (AMP-ChMic)

The MSI-78A-SH peptide was synthetized by Peptide Synthesis Facility in *Faculdade de Ciências da Universidade do Porto*. This AMP is a MSI-78 (GIGKFLKKAKKF**G**KAFVKILKK) modified peptide, an analogue of magainin-2. Its sequence is GIGKFLKKAKKF**A**KAFVKILKK-ahx-C (MSI-78A-SH), differing from MSI-78 in the substitution of a glycine by an alanine. This AMP was also modified with a terminal cysteine (C) that contains a thiol group (-SH) to enable the functionalization reaction with the MAL group of the PEG-ChMic. As PEG, ahx (aminohexanoic acid) of the AMP also acts as a small spacer to improve AMP exposure.

AMP solution was prepared in PB (pH 6.6) and added to the PEG-ChMic solution to have a final concentration of 1 mg of peptide per mL of PEG-ChMic solution. MSI-78A-SH incubation proceeded for 6 h, at RT and 150 rpm. After, the solution was filtered with an Amicon® filtration system (filter 100 kDa) and centrifuged twice at 5000 *g* for 30 min (Eppendorf 5417R, Germany). The microspheres were collected and resuspended in 1.5 mL of water type I (Milli-Q, 18.2 MΩ·cm at 25 °C; Merck Millipore, United States), and the filtered solution stored for later analysis (AMP quantification by UV/VIS spectroscopy). At the end, three types of ChMic were obtained:

1: ChMic' – Microspheres control, only treated with PB and without PEG or AMP;

2: PEG-ChMic – Microspheres only functionalized with PEG (without AMP);
3: AMP-ChMic – Microspheres functionalized with PEG and AMP.

4.4 - Microspheres Sterilization

ChMic', PEG-ChMic and AMP-ChMic solutions were transferred to a 1.5 mL Eppendorf®, centrifuged for 10 min at 10 000 g (Eppendorf 5417R, Germany) and incubated with filtered 70% (v/v) ethanol (Valente & Ribeiro, Portugal) for 30 min at 150 rpm, and then centrifuged again in the same conditions. After, microspheres' pellet was resuspended in type I water (Milli-Q, 18.2 MΩ·cm at 25 °C; Merck Millipore, United States). The solution was sonicated with the ultrasound probe VibraCelll™ (Sonics & Materials, United Kingdom) for 5 min, amplitude 70 % (Fig. 4.4). Sterility control was assessed as explained in 4.6.2.

4.5 - Microspheres Characterization

4.5.1 Fourier Transform Infrared Spectroscopy (FTIR)

The FTIR spectra were obtained using a Perkin-Elmer System 2000 FTIR spectrometer (Perkin-Elmer, US). All the samples were assessed as potassium bromide (KBr) pellets. Pellets were obtained through the mix of 2 mg of microspheres previously dried overnight at 60 °C, and 200 mg of KBr, dried at 105 °C for 24 h. The mixture was milled and placed under a press in vacuum for 2 min, and then, 1 min with a pressure of 8 tons. The infrared spectra were obtained by the accumulation of 32 scans, at 4 cm^{-1} spectral resolution, from 4000 to 400 cm^{-1}.

Chitosan degree of acetylation (DA) was calculated according to Brugnerotto method [122] (Fig. 4.2), using the 1320 cm^{-1} band (C-N stretching vibration) as the analytical, and the one at 1420 cm^{-1} (O-H deformation vibration) as the internal reference band (Eq. 4.1).

$$DA\ (\%) = \frac{A_{1320}/A_{1420} - 0.3822}{0.03133}\ , \qquad \text{(Eq. 4.1)}$$

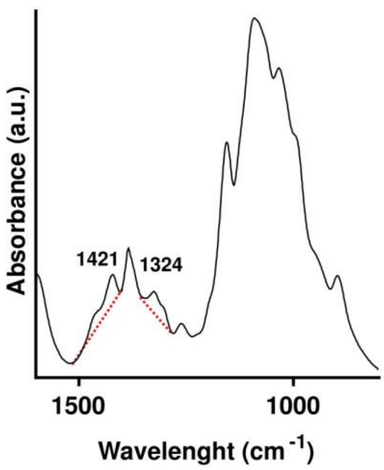

Figure 4.2 - FTIR spectrum of chitosan 6 % DA. Representation of the method used to calculate the DA of chitosan using FTIR. This method is based on the ratio between the area of the analytical 1320 cm^{-1} and internal band 1420 cm^{-1} included in the equation described above (eq. 4.1).

4.5.2 Laser Diffractometry

Microspheres size measurements were performed by Laser Diffractometry in *Faculdade de Farmácia da Universidade do Porto* using a Mastersizer 3000 (Malvern, United Kingdom) and in LEBAPE, using a Coulter-LS 230 Particle Size Analyzer (Beckman, United States). In the Mastersizer equipment, measurements were performed using tap water as dispersant and performed at RT. Samples were added until 5 % of obscuration was reached, and tested five times at 2000 rpm [123]. The absorption index and the refractive index were 0.001 and 1.4, respectively. In the Coulter equipment, measurements were performed using ethanol 70 % as a dispersant and samples were irradiated with ultrasound. The results obtained were an average of three 60-second runs.

4.5.3 Fluorescence Microscopy

Images were obtained in an inverted fluorescence microscope Axiovert 200 M (Zeiss, Germany) using a Zeiss AxioCam MRm camera and AxioVision Rel. 4.8 software. A drop of the microspheres solution was added to a microscope slide and covered with a glass coverslip. Images were acquired using the 63x immersion lens. ChMics were visualized in the DAPI channel (470 nm), as the crosslinking reaction augments chitosan autofluorescence in this wavelength [94]. Image analysis was performed using the ImageJ software (1.51j8).

4.5.4 UV/VIS Spectroscopy

The amount of immobilized peptide was determined using an UV/VIS spectrophotometer (Lambda 45; Perkin Elmer, United States). Briefly, a scan from 280 to 195 nm was made using decreasing concentrations of the MSI-78A-SH. With the absorbance value of the peak obtained at 202 nm [124], a calibration curve was made. Absorbance of the filtered solution saved in the last step of the immobilization, which contained the non-immobilized MSI-78A-SH, was measured and MSI-78A-SH concentration calculated using the previously performed calibration curve. The amount of immobilized AMP was calculated by the difference between the concentrations of the AMP solutions before and after reaction (filtered solution) with PEG-ChMic.

4.5.5 High Throughput Microscopy

Images were acquired in an IN Cell Analyzer 2000 (GE Healthcare, United States), a high throughput widefield fluorescence microscope. Samples were ultrasonicated as previously mentioned (4.4. Microspheres Sterilization) and 15 µL were added to a 96 half-wells plate (Greiner Bio-One, Austria). Images were acquired with a binning of 2x2, 2.5 D acquisition mode with a Z section of 2.5 µm with FITC filter and using a Nikon 20X/0.45 NA Plan Fluor objective. Image analysis and quantification were performed using Ilastik, a machine learning segmentation software and CellProfiler, an image processing software. Briefly, Ilastik identifies the ChMic and creates a black and white image based on the original; after, CellProfiler recognizes the ChMic, outlines and analyzes them, regarding their sizes. Every Mic outlined was analyzed and counted.

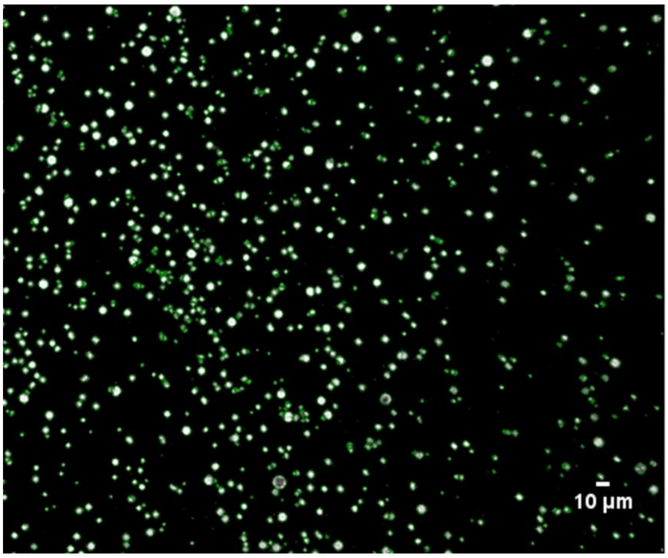

Figure 4.3 - Image of the microspheres obtained after the Ilastik and CellProfiler analysis. Microspheres are represented in white, while the outlines are represented in green.

4.5.6 Scanning Electron Microscopy

Microspheres solution was quickly frozen with liquid nitrogen, to prevent morphology loss, and freeze dried (Freezone 2.5 Plus; Labconco, Germany) for 72 h to eliminate water content. The microspheres' powder was fixed on a SEM pin with carbon tape and coated with a thin layer of gold by sputtering to improve its conductivity. Observation was performed in a Tabletop Microscope TM3030Plus, using different observation modes (5 kV/ 15 kV/ EDX) and signaling detection (Backscattered electrons, Secondary electrons, Mix).

4.6 - *In vitro* efficacy assays

4.6.1 Bacterial Growth

H. pylori solid medium plates (*H. pylori* plates) were prepared with blood agar base 2 (Liofilchem, Italy) supplemented with 0.2% (v/v) of an antibiotic cocktail composed of: 6.25 g/l Vancomycin (Sigma-Aldrich, United States), 3.125 g/L Trimethroprim (Sigma-Aldrich, United States), 0.155 g/L Polymixin B (Sigma-Aldrich, United States) and 1.25 g/L Amphotericin B (Sigma-Aldrich, United States); plus 10% (v/v) defibrinated horse blood (Probiológica, Portugal). The liquid media used was Brucella broth (BB; Fluka, Switzerland) supplemented with 10 % (v/v) of heat inactivated fetal bovine serum (FBS; Gibco, United States).

The human *H. pylori* strain J99 (obtained from the Department of Medical Biochemistry and Biophysics, Umeã University, Sweden) was used in the herein reported assays.

H. pylori J99 was cultured in spots (20 µL per spot, 4 spots per plate) in *H. pylori* medium plates, for 48 h, at 37 °C in a microaerophilic environment (GENBox Microaer system; BioMérieux, France). After, some colonies were selected and spread on *H. pylori* medium plates, and incubated in the same above-mentioned conditions for 48 h. Then, bacteria were transferred to a 25 mL T-flask (SPL, Korea), containing liquid medium (BB + 10% FBS). The OD was adjusted to 0.1, ʎ = 600 nm (Lambda 45, Perkin Elmer, US). *H. pylori* was incubated at 150 rpm, 18-20 h, 37°C and under microaerophilic conditions for the following experiments.

For all the experiments, bacterial OD was adjusted to 0.03, which corresponds to a concentration of $1x10^7$ CFU per mL, in accordance to previous works [125] and following the CLSI guidelines [126]. The initial inoculum was plated in *H. pylori* plates to confirm the CFU/mL.

4.6.2 Sterility Control

Microspheres sterility was accessed by 24 h incubation at 37 ºC in bacterial medium, either TSB (Merck, Germany), a general growth media; or BB + 10 % FBS, more specific towards *H. pylori* growth, under a microaerophilic environment (GENBox system; BioMérieux, France). Sterility was confirmed by naked eye visualization (no alterations in turbidimetry). However, in the cases where naked eye observation was doubtful, platting in TSA (Sigma-Aldrich, United States) was performed to confirm sterility. Microspheres morphology, as well as aggregation after sterilization were assessed by high throughput microscopy as mentioned in 4.5.5.

4.6.3 Antibacterial Performance in Phosphate Buffered Saline

The ability of AMP-ChMics to interfere with *H. pylori* growth was firstly accessed in PBS (pH ~7.4), after 30 min, 2 h and 6 h of incubation. The bacteria pre-inoculum (4.6.1) was centrifuged twice at 2700 rpm for 5 min (in order to remove the liquid medium) and then bacterial pellet was resuspended in PBS. The selected microspheres concentrations were $10^5/10^4/10^3$ (ChMic/mL). For the three time points and all concentrations tested, serial dilutions were performed and plated in *H. pylori* plates for colony forming units (CFU) counting. CFU were determined after 5 days incubation at 37ºC, under microaerophilic conditions. In parallel, the presence of metabolic activity was also accessed by the thiazolyl blue tetrazolium bromide (MTT) method [111]. The MTT is a yellow reagent that when metabolized by active cells/bacteria is reduced and turns its color to purple, allowing visual determination of metabolic activity. MTT was added in a final 0.2 mg/mL concentration as described elsewhere [127]. Also, ChMic' and PEG-ChMic (controls) were incubated in the exact same conditions as the AMP-ChMic, as well as pure *H. pylori* (without any type of microspheres). After the above-mentioned time points, all the conditions were plated in *H. pylori* plates. As a control of sterility, microspheres were incubated only with PBS.

4.6.4 Antibacterial Performance in Culture Medium

The same procedure used in the PBS assays (4.6.1) was used to assess the antibacterial activity of the microspheres in BB + 10 % FBS. However, more concentrations of AMP-ChMic (10^4-10^7) were tested since culture medium favors *H. pylori* growth. As a control of sterility, microspheres were incubated only with BB + 10 % FBS.

4.6.5 Statistics

To determine statistically significant differences regarding the number of viable bacteria, T-test was used and differences were considered statistically significant for $p < 0.05$ (GraphPad Prism 5 software).

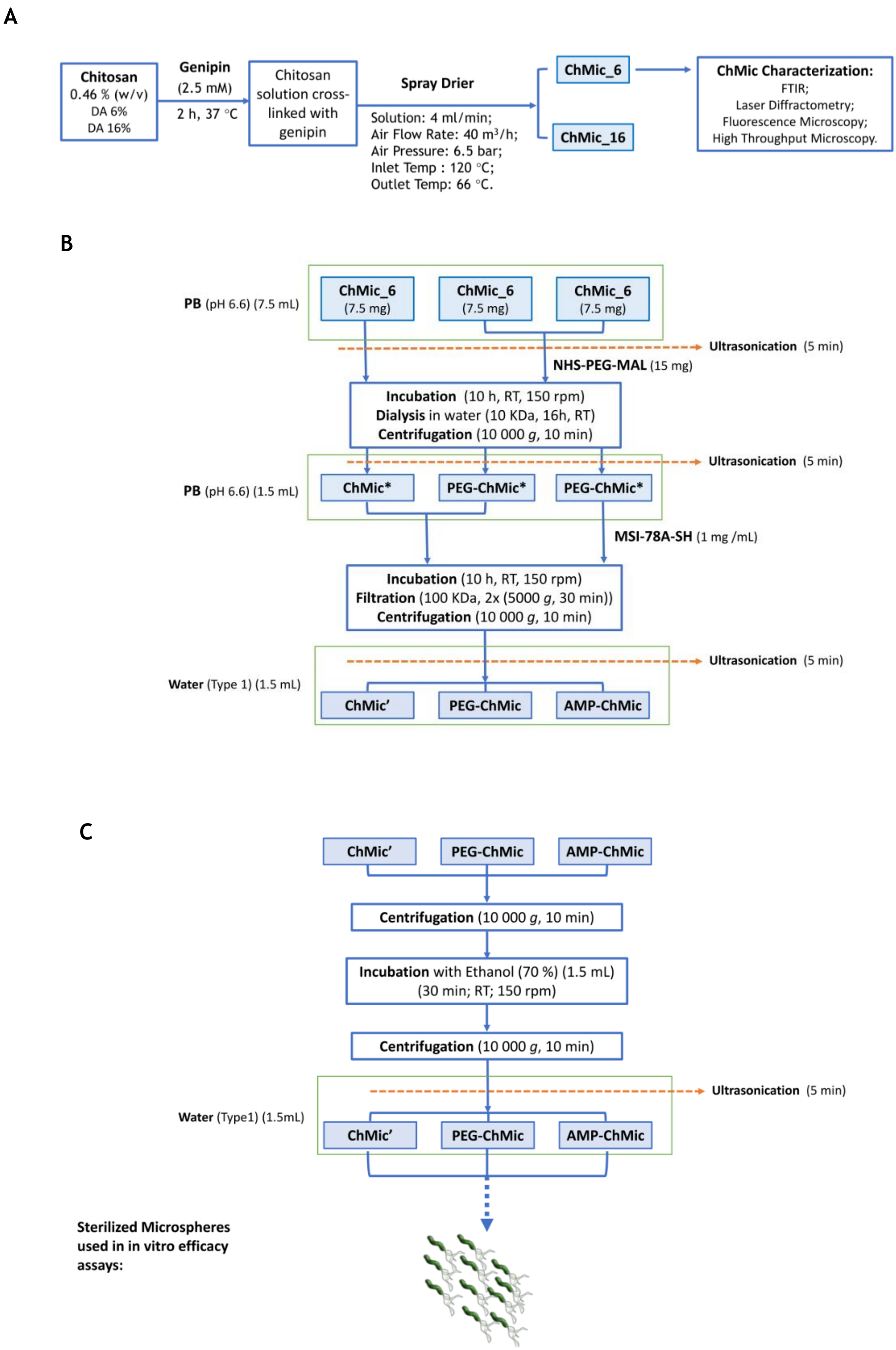

Figure 4.4 - Schematic representation of the steps preformed to obtain AMP-ChMic for the *in vitro* assays. A- Microspheres production; B- Functionalization; C- Sterilization.

Chapter 5

Results and Discussion

5.1 - Chitosan Microspheres (ChMic) Preparation

5.1.1 Chitosan Purification

Two different commercial chitosan powders, with DA 6 % and 16 %, were purified and characterized by FTIR.

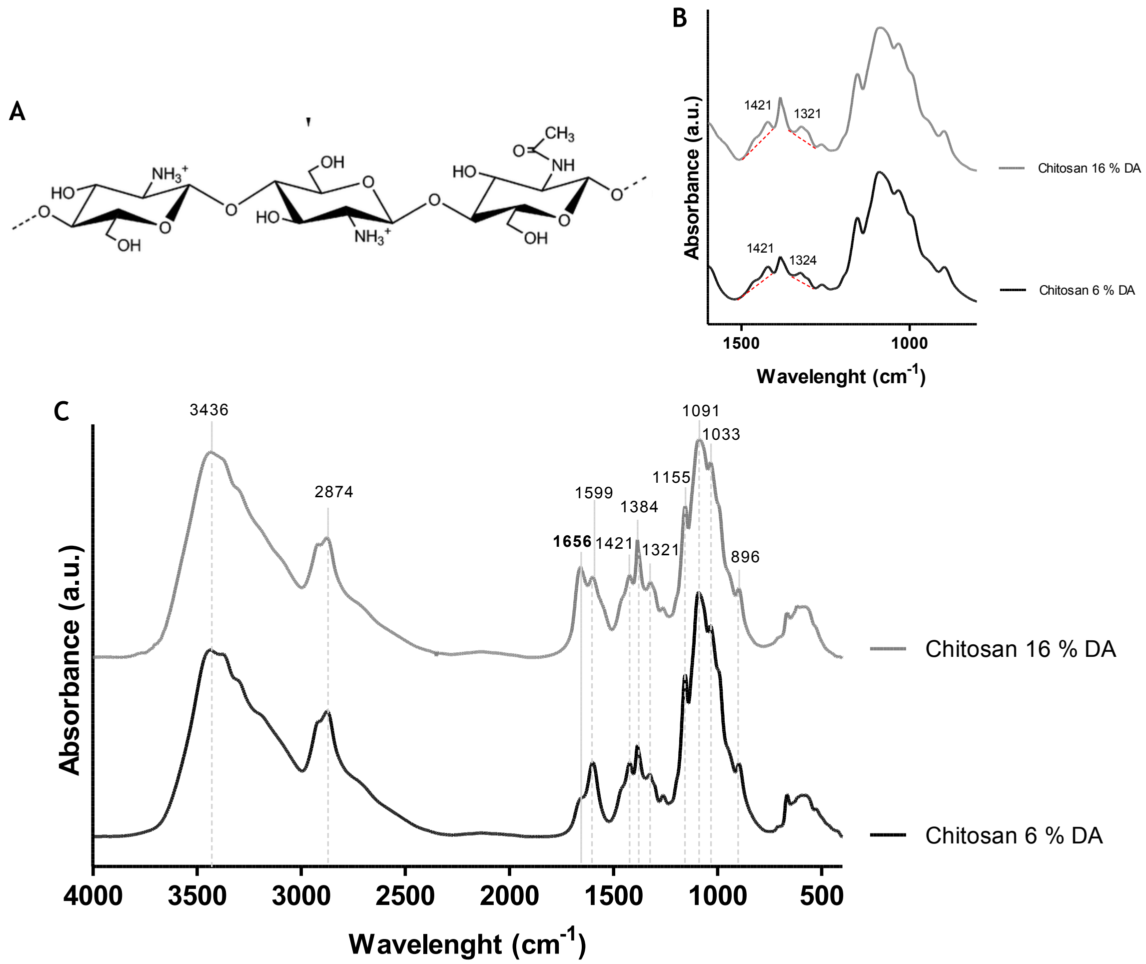

Figure 5.1 - A- Chitosan chemical structure; B- Region of chitosan FTIR spectra that was used for DA calculation; C- Full FTIR spectra of chitosan with DA 6 and 16 %.

FTIR spectra of chitosan, as well as its chemical structure are presented at Fig. 5.1. Both spectra (Fig. 5.1 C) present the characteristic absorption bands of pure chitosan, which suggests that purification was successful. The large absorption peak at 3500-3200 cm^{-1} corresponds to the different hydrogen vibrations. The C-H stretching is represented at 2874 cm^{-1} while 1599 cm^{-1} is relative to the amide II and the N-H bending of primary amines. The 1384 cm^{-1} is related to CH_3 symmetric deformation and the 1322 cm^{-1} corresponds to C-N stretching and N-H in plane deformation [128]. At 1421cm^{-1} there is a peak characteristic of a primary alcohol. At 1033 cm^{-1} there is a stretching vibration of C-O-C glucopyranose ring and at 1155 and 897 cm^{-1} a double peak corresponding to the β(1-4) glycoside bridge [129]. Both spectra present all the peaks above mentioned. Also, the spectrum of chitosan 16 % DA presents a more intense peak at 1656 cm^{-1}, amide I (C=O stretching from secondary amides) than the spectrum relative to chitosan 6 % DA, where it is almost absent. This is related to the fact that chitosan 6 % DA has a lower number of acetylated amine groups and higher number of primary amines (-NH_2). Chitosan DA was calculated using the Brugnerotto method [122] that uses the area of the peak at 1320 cm^{-1} (C-N stretching vibration) as the analytical band and the peak at 1420 cm^{-1} (O-H deformation vibration) as internal reference and equation 4.1 described at Material and Methods section. The spectra used for DA calculation is represented in Fig. 5.1.B.

5.1.2 Crosslinking

To prevent ChMic from degradation in the stomach acidic conditions (pH ~1.2), it was required to add a crosslinking agent prior to microspheres preparation by spray drier technique. Although the most common agent is glutaraldehyde, genipin was the crosslinking agent selected in this work due to its lower cytotoxicity [82]. Crosslinking degree, which is related with the amount of genipin that covalently binds to chitosan (Fig. 5.2), was optimized by changing different parameters, namely: genipin concentration, temperature and reaction time (Table 4.1; see Material and Methods section). For crosslinking optimization purposes, only Ch 16 % DA was used.

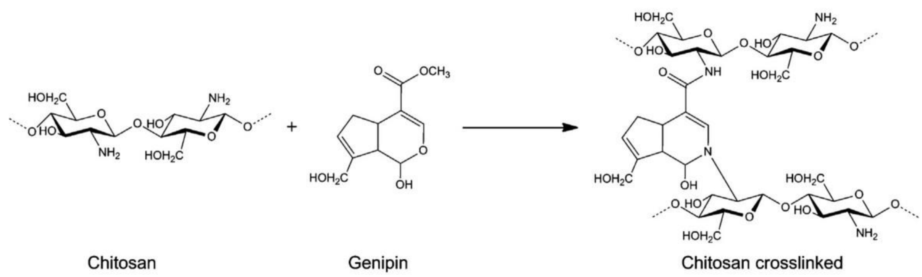

Figure 5.2 - Chitosan and genipin reaction. Adapted from Fernandes *et al.* [94]

During the crosslinking reaction, the solution color changes from transparent to blue, appearing the blue pigments as a result of the oxygen radical-induced polymerization of genipin that occurs when a heterocyclic compound is formed in the chitosan/genipin reaction [83,87,130]. Previous studies made in our group (unpublished data) tested different genipin concentrations and incubation time, establishing that 2.5 mM genipin for 2 h at 37 °C were the ideal conditions for ChMic production by the spray drying technique. However, Harris *et al.* reported 50 °C as the best temperature to perform this crosslinking reaction [131]. To understand how the alteration of temperature and reaction time could be used to decrease genipin concentration, the crosslinking reaction was tested at 37 °C (A), and 50 °C (B, C, D and E). Different genipin concentrations were also tested (2.5, 1.0, 0.5 and 0.25 mM) as well as incubation time, ranging from 2 h up to 24 h. The parameters chosen took into account previous reports that changing some conditions, namely less genipin for 24 h at 37 °C, would lead to microspheres dissolution and aggregation in acidic medium. Differences between the solutions were evaluated by color alteration and assessing the viscosity, since an increase on the viscosity of chitosan solution with the addition of genipin is expected [130].

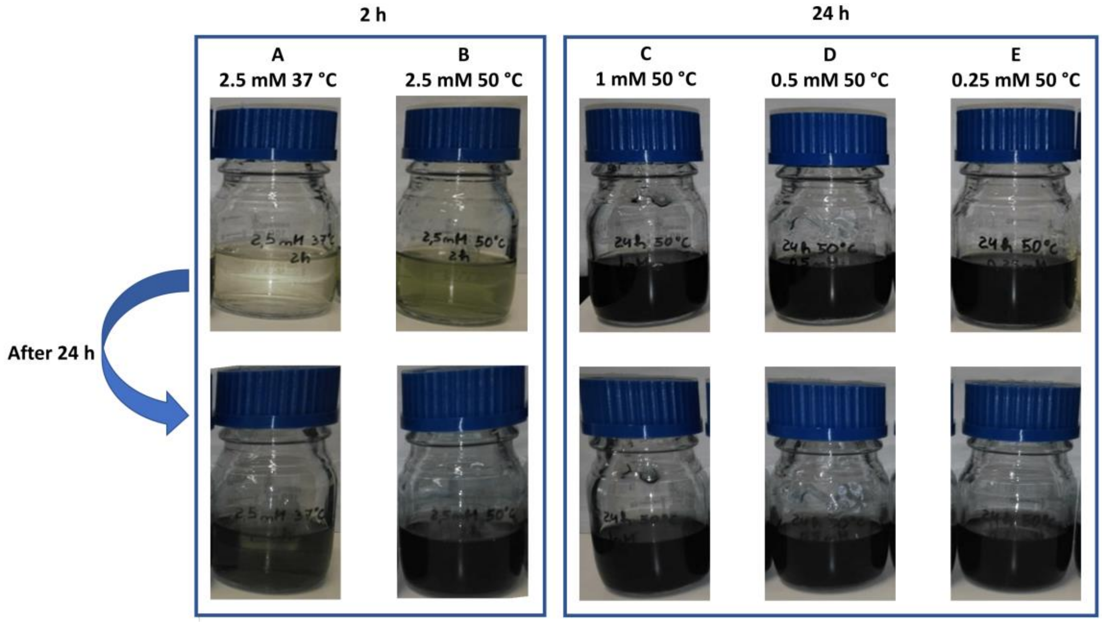

Figure 5.3 - Chitosan crosslinked with genipin (above) and after more 24 h (below).

After 2 h of incubation, samples A and B presented a slight color change, indicating that the crosslinking reaction had begun. The other samples, incubated for 24 h (samples C, D and E) presented a blue shade, suggesting that the reaction was complete. The fact that the chitosan solution of samples A and B did not reach a blue color suggested that the crosslinking reaction was still undergoing. Therefore, samples A-E were maintained for an additional 24 h at RT to evaluate if differences in both color and viscosity occurred. Color wise, C, D and E samples did not undergo any naked eye changes, which may indicate that after 24 h of incubation the crosslinking reaction was complete, while A and B turned blue (Fig. 5.3). Solutions were evaluated using rheometry after the crosslinking time indicated in Table 4.1, as well as after the additional 24 h period, but no significant differences in viscosity were detected between different samples (results not shown). For microspheres production by spray dryer, an incomplete crosslinked solution is desired, since it will allow the crosslinking reaction to proceed inside the microsphere after their production, which will then avoid the microspheres dissolution in acidic conditions. If crosslinking was completed before the spray dryer process, only physical forces would maintain microspheres integrity, which would not be strong enough and would cause microspheres to collapse in acidic solutions. Assays performed at 50ºC increased the color of the solutions in comparison with the control (Condition A at 37ºC), suggesting a more complete crosslinking process. Therefore, microspheres used in this work were prepared using the following conditions: 2.5 mM genipin, 37 °C, 2 h (Condition A), as previously described by our group.

5.1.3 Spray Drying

The production of the microspheres was done using a spray dryer equipment. Some of the major advantages of the spray drying technique are its easiness to work with, the inexpensiveness, and the fact that it has been extensively studied [121]. Although being described to have low yields in a laboratory scale, its average yield increases in industrial productions, which makes it an ideal production method when the scale up process is envisioned [132]. Another frequently used technique to produce ChMic is the ionic gelation method, but this is considered a slow process and the obtained ChMic, only crosslinked by electrostatic interactions, have poor stability in acidic conditions [82]. Moreover, spray drying technique allows the manufacturing of microspheres with controlled sizes. In this work, it was desired to obtain microspheres with sizes ranging from 2-4 µm, as it was anticipated that it would allow a more close and direct contact with bacteria. ChMic were prepared using chitosan with DA 6 % (ChMic_6) and 16 % (ChMic_16). The efficiency of the production of ChMic_6 and ChMic_16 was 39 % and 38 %, respectively. A FTIR analysis was performed to check if, after the spray drying process, the ChMic retained the chitosan characteristic peaks and if it was possible to detect genipin crosslinking (Fig. 5.4).

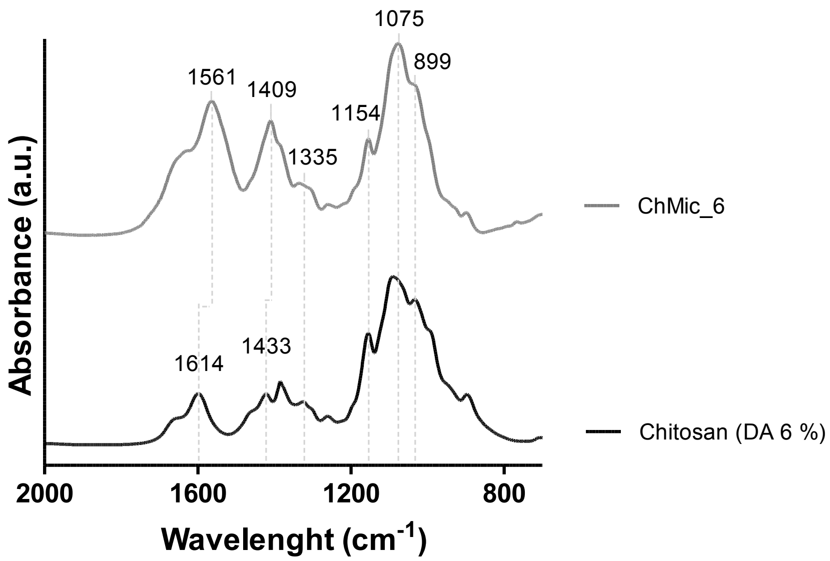

Figure 5.4 - FTIR spectra ChMic_6 vs Chitosan (DA 6%).

The FTIR spectrum of ChMic_6 presented the same peaks as the Chitosan spectrum (DA 6 %), although some peaks were slightly shifted to the right, namely the ones at 1409 and 1561 cm^{-1} (Fig. 5.4). The peak at 1409 cm^{-1} increased when compared with the 1154 cm^{-1} from the chitosan glycoside bridge. This increase in the intensity is due to the ring stretching of the genipin molecule and is in accordance with what was described by Fernandes *et al.* [94].

Laser diffractometry was used to measure the ChMic size. This technique uses the diffraction patterns created by an object passing through a laser beam, since the pattern varies with the size of the objects. The obtained results are concordant and point to the desired size distribution, having 80% of the ChMic with diameters between 2.50 and 7.21 μm (Fig. 5.5 A and B).

A

B

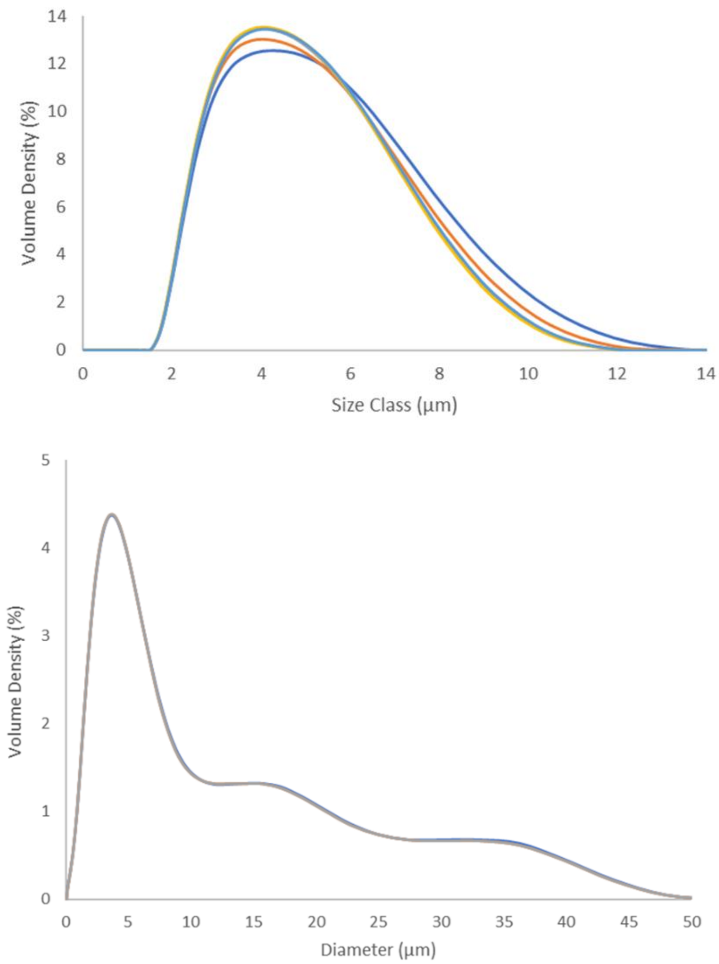

Dv 10	Dv 50	Dv 90
	(μm)	
2.50	4.21	7.21

Average (μm)
6.25

Figure 5.5 - Size distribution of the microspheres. A- Analysis performed in the Mastersizer 3000 equipment; B- Analysis performed in the Coulter LS 230 equipment.

The higher values (> 7.21 μm) seen in Fig. 5.5 B correspond to particle aggregates, especially because this analysis was performed in ethanol, in which microspheres have tendency to aggregate. The size range of particles obtained by spray drying technique varies accordingly to the fabrication settings, as well as intrinsic solution characteristics [121]. For instance, when glutaraldehyde is used as crosslinking agent, chitosan with higher molecular weight suffers a faster gelification process, leading to higher surface roughness and lower particle size [121]. Particle size increases with the increase in viscosity and surface tension of the initial solution [133]. With this technique it is possible to produce particles that can vary from few micrometers to approximately 3 millimeters [133]. The herein obtained results are in agreement with previous reports, as Lopes *et al*. obtained, in similar experimental conditions, average diameters of 6.03 μm [134].

SEM analysis revealed that ChMic, after spray drying production, are spherical and present slight surface roughness (Fig. 5.6). Some ChMic aggregated after production, as excepted in dry conditions, possibly due to electrostatic interactions [135]. This analysis also confirms the variation in microspheres size previously described when using other size measurements techniques.

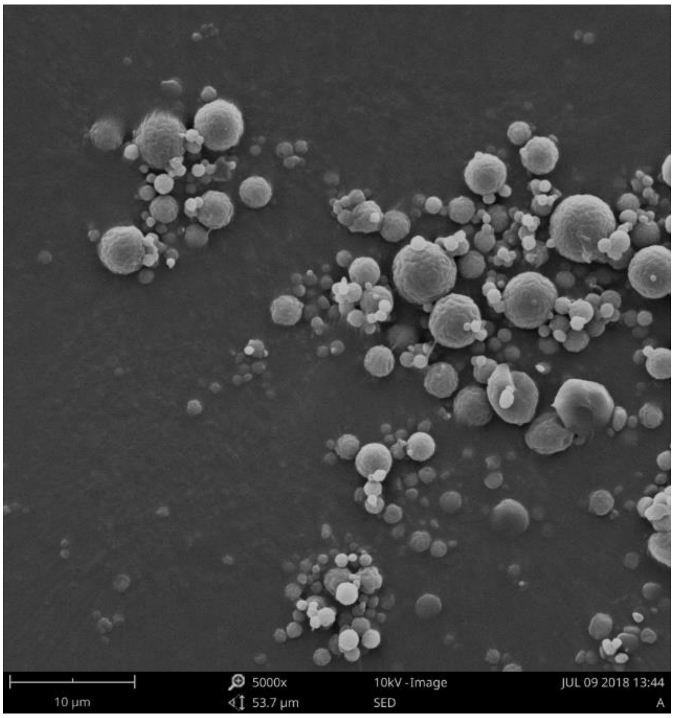

Figure 5.6 - Scanning Electron Microscopy of Microspheres (5000x).

5.1.4 Stability

In order to test ChMic stability in low pH, mimicking the stomach pH, incubation in an acidic medium (citrate-phosphate buffer, pH 2.6) was performed [136]. In addition, and since it was previously observed that ChMic had tendency to aggregate, their ability to disperse in solution was evaluated using different sonication methods, namely ultrasound bath and ultrasound probe. ChMics retained their integrity at both pH 2.6 and in type II water (pH 7). The ultrasound probe was more efficient than the ultrasound bath in diminishing the ChMic aggregation. After 5 min in the ultrasound probe with 70 % amplitude, ChMic were disaggregated and dispersed in solution (Fig. 5.7).

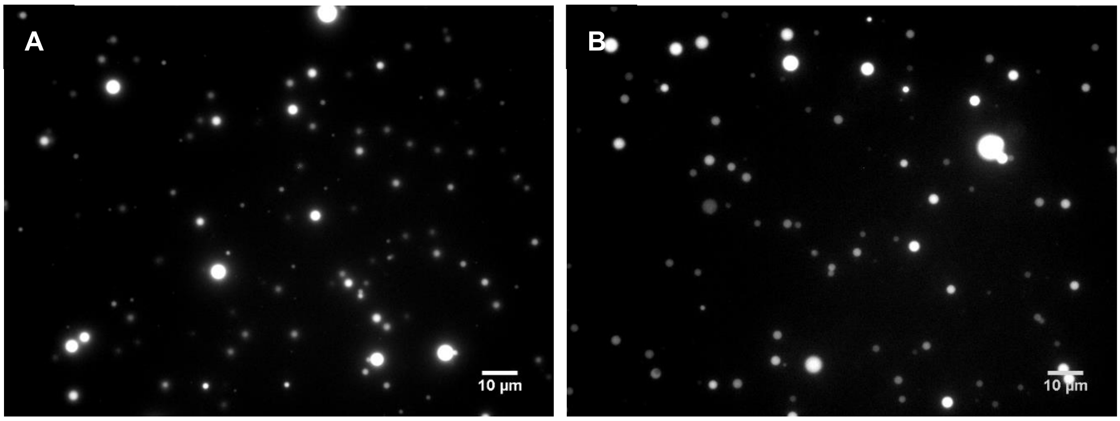

Figure 5.7 - Microspheres after 5 min in the ultrasound probe. (Inverted Fluorescence microscopy; 630 x magnification). A- Water; B- Citrate-phosphate buffer pH 2.6.

5.2 - Microspheres Functionalization

5.2.1 PEG and AMP Immobilization

MSI-78A-SH immobilization on the surface was performed using a bifunctional PEG as a spacer, to favor AMP exposure from the ChMic surface and thus, improve its bioactivity when immobilized on the microsphere. This highly hydrophilic molecule provides more mobility to the AMP, decreases non-specific binding and can be functionalized to react with different chemical groups [137]. In this work, PEG with NHS and MAL terminal groups was chosen, for the NHS to react with the free amines from chitosan and the MAL to react with terminal cysteine from the AMP. To maximize the linkage between the amine groups and NHS, PEG was added sequentially over the incubation time period. Then, AMP was immobilized via its terminal cysteine that reacts with the double bond in the MAL ring. The addition of the AMP had to be 'fast' to prevent that MAL group would undergo degradation. A similar chemistry was attempted by Wu *et al.*, for the immobilization of cecropin P1 (CP1) AMP on silica nanoparticles [138]. One of the aims of Wu's work was to assess the effect of different PEG chain lengths on the antimicrobial activity of CP1 against *E. coli*. It was reported that the MIC values were inferior for the higher PEG chain length tested – $(PEG)_{20}$, with a chain of twenty ethylene glycol groups. PEG used in this dissertation had a chain twelve ethylene glycol groups ($(PEG)_{12}$) and was chosen based on previous work carried out in our team that considered this PEG length long enough to allow good AMP exposure.

ChMic functionalization was followed by FTIR (Fig. 5.9).

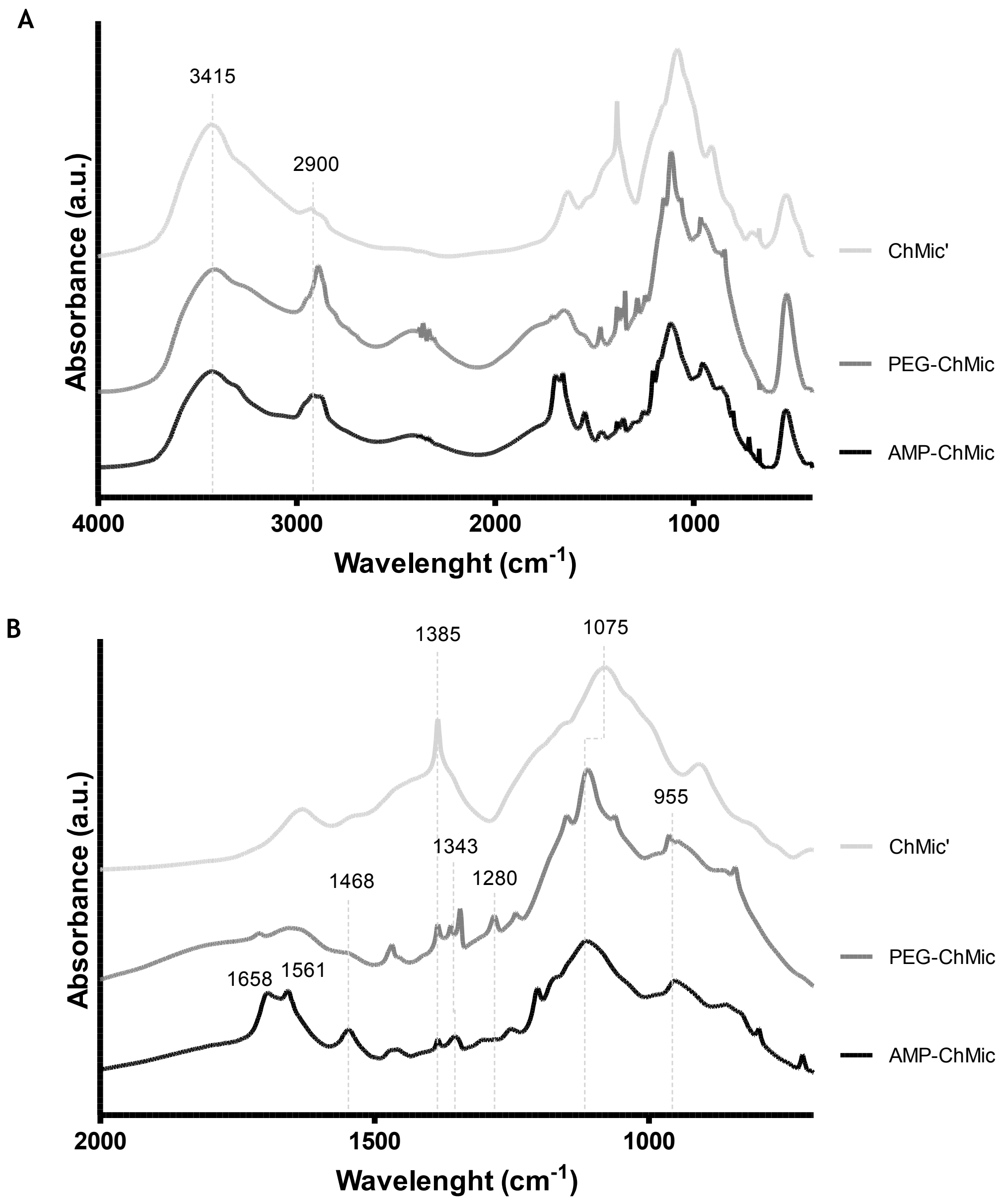

Figure 5.8 - FTIR spectra of ChMic', PEG-ChMic and AMP-ChMic in the region of A- 4000 cm^{-1}- 400 cm^{-1} and B- 2000 cm^{-1}- 700 cm^{-1}.

Comparing the ChMic' with PEG-ChMic spectrums, new peaks were observed after PEG addition (Fig. 5.9). PEG-ChMic exhibits the characteristic absorption bands of ChMic' and an extra peak at 2900 cm^{-1} that is assigned to the carbonyl chain (-CH) of PEG (Fig. 5.9A). Fig. 5.9B shows that the peak at 1075 cm^{-1} observed at ChMic' suffered a shift to 1111 cm^{-1} in the PEG-ChMic, as a result of the -C-O-C stretching vibration on the spacer's straight chain instead of the chitosan's glucopyranose ring [139]. Moreover, other PEG characteristic peaks such 1280 cm^{-1} from CO, 1343 cm^{-1} from C=O and 955 cm^{-1} from CH=CH are present at PEG-ChMic spectrum [140] demonstrating that PEG was successfully immobilized onto ChMic'. Concerning AMP-ChMic spectrum, the increase of the peak at 1658 cm^{-1} that is assigned to the amide I ($-CONH_2$)

characteristic of peptides [141], indicates the presence of MSI-78A-SH. These results indicate that the AMP immobilization was successful.

Through fluorescence microscopy it was possible to observe that the ChMic maintained their integrity after AMP immobilization (Fig. 5.10). Although all developed microspheres (ChMic', PEG-ChMic and AMP-ChMic) need to undergo ultrasound probe dispersion, AMP-ChMic have less tendency to aggregate than the others. This can be due to electrostatic repulsions between the positively charged MSI-78A-SH immobilized on the microspheres' surface.

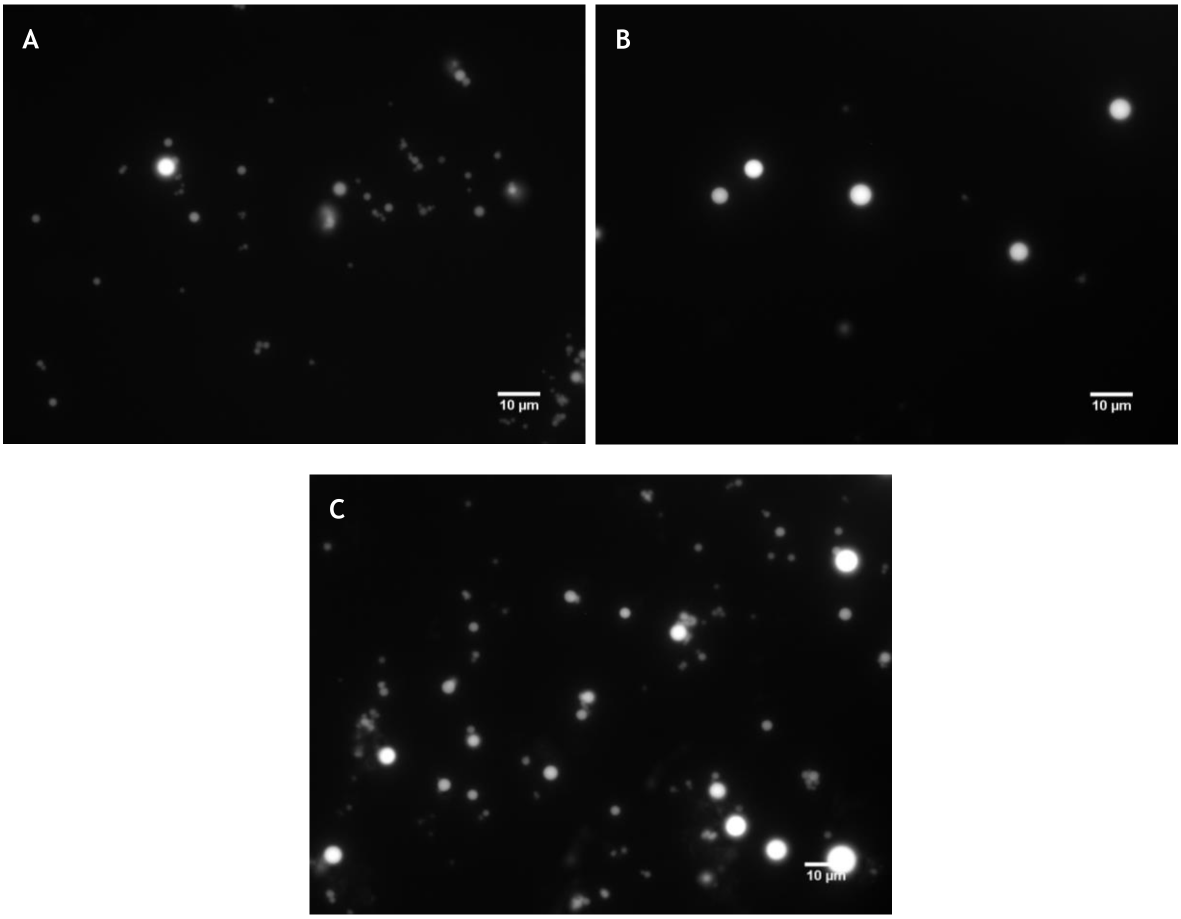

Figure 5.9 - Microspheres in water after 5 min of ultrasonication (Inverted fluorescence microscope, magnification 630 x) A- ChMic'; B- PEG-ChMic; C- AMP-ChMic.

5.2.2 AMP Quantification

AMP immobilization yield was calculated in solution using UV/VIS spectroscopy, by the difference between the absorbance of the initial AMP solution (1000 µg/mL) and the absorbance of the solution recovered after AMP immobilization (solution recovered after filtration and washing process). A calibration curve was done using increasing concentrations of MSI-78A-SH, from 1.95 to 500 µg/mL. The calibration curve was built based on the absorbance of the AMP sample at 202 nm, in accordance to what was reported in the literature [124]. Based on the analysis of the recovered solution, the concentration of AMP unbound to the microspheres was 179.8 µg/mL. The yield of the immobilization was 82 %, with 820 µg/mL of AMP present on the AMP-ChMic solution. It can be estimated that each microsphere has approximately 6.3×10^{-6} µg of AMP on its surface. However, it is probable that not all the microspheres possess the same amount of AMP, and that some have more immobilized AMP than others, which can be related with the size distribution in the sample. To further evaluate and improve the AMP immobilization, different AMP concentrations could be tested, and analyze how it would impact the immobilization yield [111]. Those results would be important to give a clear indication of the best formulation conditions.

5.2.3 Sterilization

All the Mics (ChMic', PEG-ChMic, AMP-ChMic) needed to undergo a sterilization procedure prior to *in vitro* activity assays. Based on the literature, ethanol 70% (v/v) was selected as the sterilization method [142]. An important parameter to be taken into account was that Mics integrity was kept during ethanol 70% (v/v) sterilization. Also, although Mics tend to aggregate in ethanol 70%, this was overcome once Mics were after transferred to water and subjected to probe ultrasonication. Altogether, it was demonstrated that Mics could be sterilized using this procedure without compromising the obtained Mics.

5.2.4 Microspheres Quantification

Prior to *in vitro* assays, it was necessary to quantify the microspheres (number of Mics per mL solution). Quantification was performed resourcing to high throughput microscopy. Mics concentration was measured before and after AMP functionalization, as well as after sterilization (Table 5.1). Interestingly, an increase in the microspheres number after AMP immobilization and after sterilization was observed. This was not expected and so, alteration in Mics size was evaluated using this technique to understand if the differences could be attributed to less particle aggregation, or particle breakage (Fig. 11). Results demonstrated that ChMic diameters are maintained after PEG and AMP immobilization. These results are in accordance to what was anticipated due to the PEG and AMP small size in comparison to ChMic' size. However, after sterilization, the AMP-ChMic had an average diameter of 2.36 µm, which is much inferior when compared with the other samples. This could be related with electrostatic repulsion between the positively charged AMP-ChMic, an effect that could be further enhanced by sterilization, which will then reduce the amount of aggregates, and thus reduce the overall average diameter. This also explains the subtle 'growth' in the number of AMP-ChMic after sterilization and when compared with the other conditions, as the higher number of Mics is most likely due to fewer aggregates and more 'free' microspheres.

Table 5.1 – Mic quantification along after the production, functionalization and sterilization.

Steps	Samples	Concentration (Mic/mL)
Production	ChMic	1.37×10^8
Functionalization	ChMic'	3.68×10^7
	PEG-ChMic	4.22×10^7
	AMP-ChMic	8.64×10^7
Sterilization	ChMic'	2.45×10^7
	PEG-ChMic	4.80×10^7
	AMP-ChMic	1.82×10^8

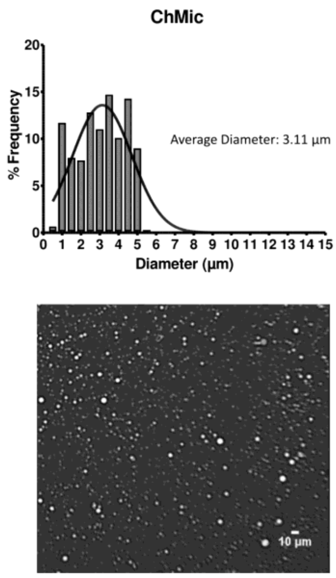
ChMic
% Frequency
Average Diameter: 3.11 µm
Diameter (µm)
10 µm

B

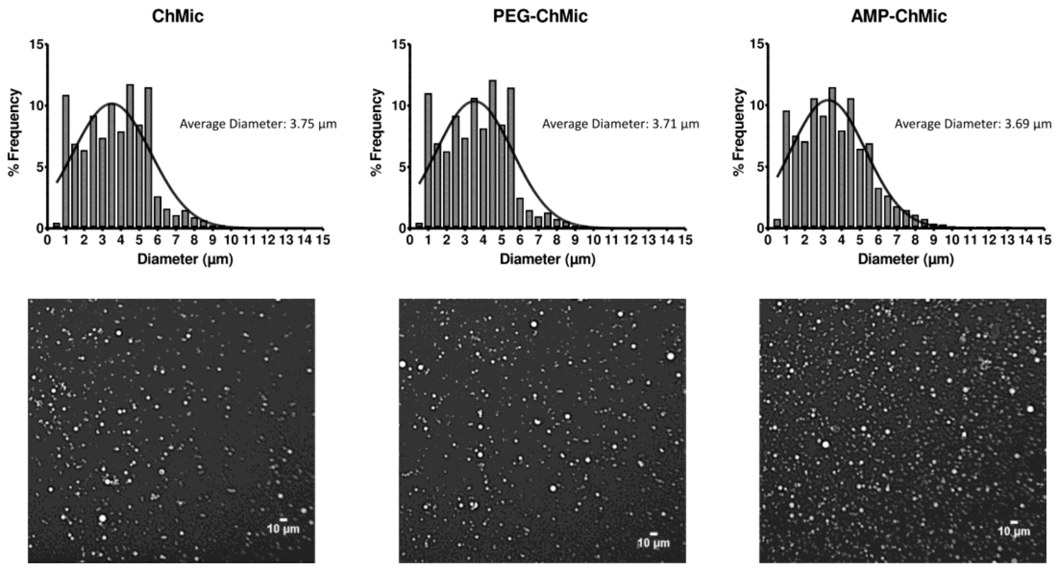
ChMic
PEG-ChMic
AMP-ChMic
% Frequency
Average Diameter: 3.75 µm
Average Diameter: 3.71 µm
Average Diameter: 3.69 µm
Diameter (µm)
10 µm

C

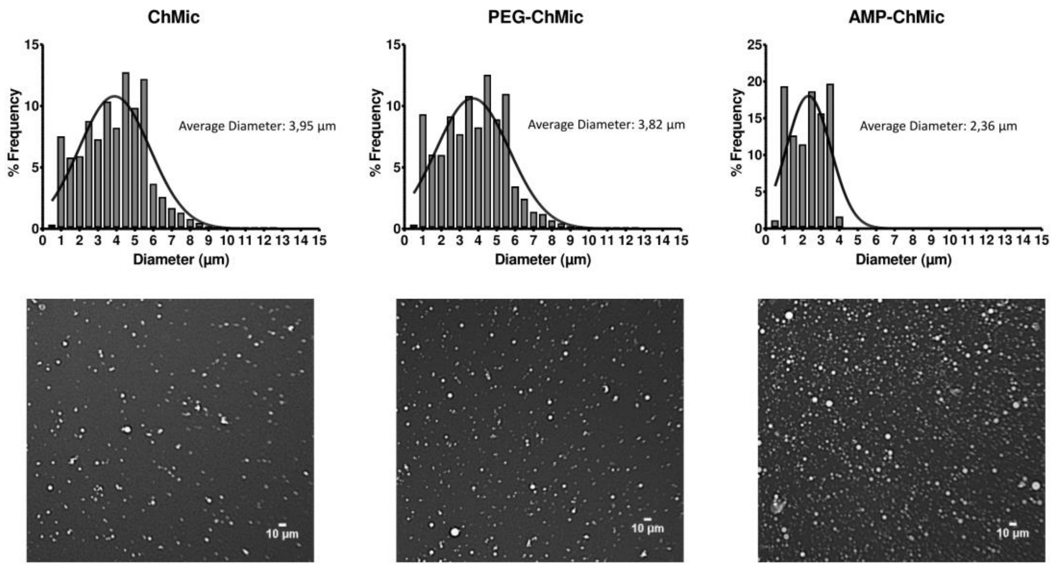
ChMic
PEG-ChMic
AMP-ChMic
% Frequency
Average Diameter: 3,95 µm
Average Diameter: 3,82 µm
Average Diameter: 2,36 µm
Diameter (µm)
10 µm

Figure 5.10 - Quantification and size distribution of the microspheres. A- ChMic' after production by spray drying, B- Mics after functionalization; C- Mics after sterilization.

5.3 - AMP-ChMic *in vitro* performance against *H. pylori*

5.3.1 Sterility control

Microspheres sterility was assessed prior to incubation with bacteria. Results did not show microbial growth, neither in liquid culture (TSB), nor plated in TSA. These results indicated that microspheres were sterile and ready to undergo *in vitro* assays. Additionally, in every assay sterility was also controlled, as microspheres alone were incubated in PBS or BB, for the whole duration of the experiment. Sterility was accessed with MTT assay.

5.3.2 *In vitro* Assays in Phosphate Buffered Saline

As a first approach, *in vitro* assays were performed in PBS. Although bacteria do not thrive in this medium, PBS was firstly used to access if the obtained Mics had any effect against this gastric pathogen. Fig. 5.12 shows the CFU counting for the *H. pylori* J99 strain incubated with different microspheres concentrations.

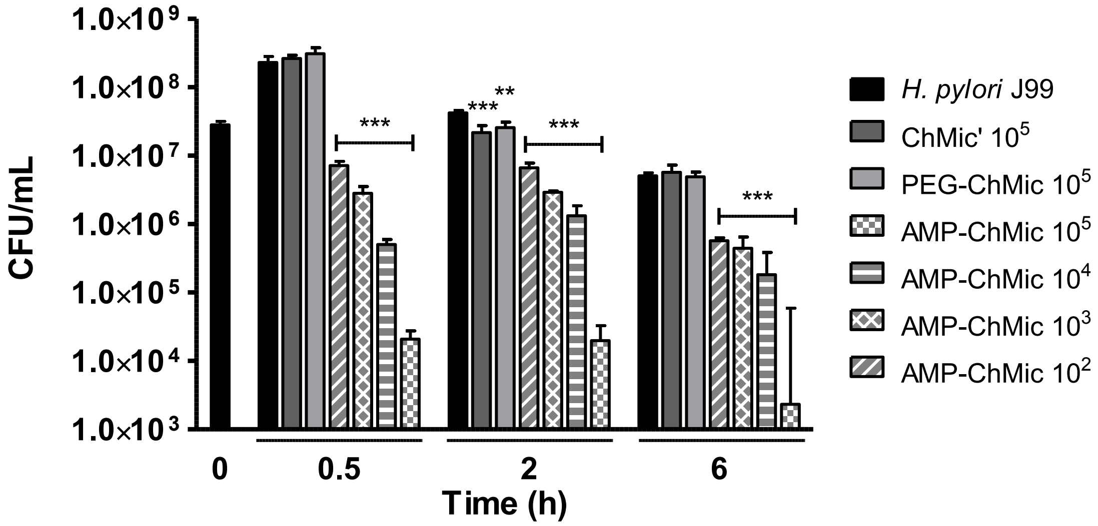

Figure 5.11 - *H. pylori* growth after 0, 30 min, 2 and 6 h of incubation with PBS. ** Statistically significantly different from *H. pylori* in the same time point. *** Statistically significantly different from *H. pylori* in the same time point (t-test; P < 0.0001).

In this assay, *H. pylori* growth was assessed at three different time points: 30 min and 2 h, because it is reported that AMP have a fast killing effect; and 6 h, as it is the reported *H. pylori* duplication time in favorable environment [125]. The CFU counting demonstrated the ability of AMP-ChMic to kill *H. pylori*. As expected, these results were better when higher concentrations were used. The higher concentration, 10^5 AMP-ChMic/mL, was able to reduce the number of bacteria present in 99.99 % after 6 h, demonstrating their strong bactericidal effect. Even the lower concentrations tested (10^4-10^2 ChMic/mL) induced death, as there was a reduction in the number of CFU. Even though at 2 h the results from the controls (ChMic' and PEG-ChMic) are statically significant, there is not a bactericidal effect, as shown in the AMP-

ChMic sample (> 3 logs of reduction). Moreover, this effect was not observed after 6h of incubation, being only visible for AMP-ChMic. Also, microspheres were incubated with PBS to ensure sterility. The observed fast bactericidal effect associated with the fact that bacteria were not affected by the control conditions, indicates that MSI-78A-SH is capable of retaining its bactericidal activity when immobilized on microspheres.

Along with the CFU counting, bacteria's metabolic activity was also assessed, through the MTT assay. This is a colorimetric assay and changes color when there is metabolic activity, MTT is enzymatically reduced to formazan, changing its color from yellow to purple. No color changes were observed, as the reagent maintained its yellow tonality. MTT assay was negative for all the samples (even the control without Mic) indicating the lack of metabolic activity. However, CFU counting demonstrated the presence of *H. pylori* viable cells. A possible explanation for this observation is the conversion of the bacteria from the more active spiral shape to coccoid form in PBS. *H. pylori* is able to convert to coccus to overcome harsh environments, such as nutrient privation in PBS, and to return to its more virulent spiral morphology when the surroundings are more appropriate [17]. In coccoid shape, *H. pylori* has minimum metabolic activity, being described as viable but in a dormant state [143]. These results support this hypothesis, as bacteria in PBS demonstrated no activity (MTT assay), but when plated in a favorable medium, *H. pylori* was able to grow and duplicate.

5.3.3 *In vitro* Assays in Culture Medium

The activity of *H. pylori* was evaluated in BB + 10 % FBS using the procedure described in 4.6.4. In this assay, bacteria were incubated in an enriched medium, favorable for thriving, and therefore it was expected that higher microspheres concentrations would be required to induce the same killing effects as those observed in PBS.

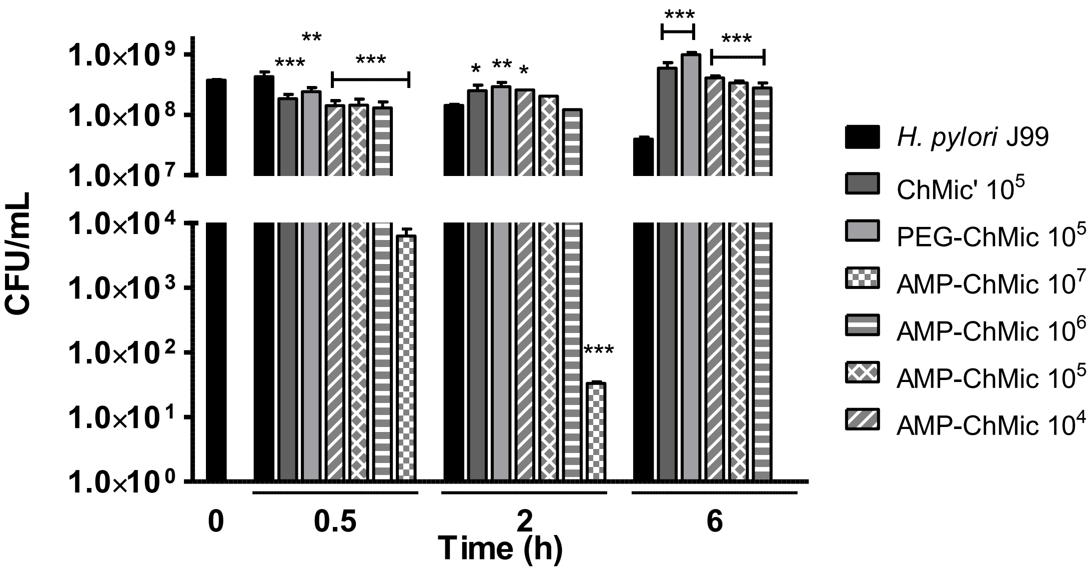

Figure 5.12 - *H. pylori* growth after 0, 0.5, 2 and 6 h of the incubation with BB + 10 % FBS (preliminary results). * Statistically significantly different from *H. pylori* in the same time point (t-test; $P < 0.05$). ** Statistically significantly different from *H. pylori* in the same time point. *** Statistically significantly different from *H. pylori* in the same time point ($P < 0.0001$).

The results shown in Fig. 5.13 highlight that the higher concentration of AMP-ChMic used, 10^7 AMP-ChMic/mL, was able to reduce the number of *H. pylori* cells within 30 minutes of incubation. The lower concentrations tested (10^6, 10^5 and 10^4 Mic/mL), showed no effect at 30 min of exposure when compared to controls. After 2 h of incubation, the number of bacteria incubated with 10^7 AMP-ChMic/mL continued to decrease, while bacteria exposed to the lower concentrations were able to grow. After 6h, no viable bacteria were detected when incubated with 10^7 AMP-ChMic/mL. Lower concentrations of AMP-ChMic showed no effect upon bacterial growth. The CFU counting was confirmed with the MTT assay. 10^7 AMP-ChMic/mL was the concentration required to effectively kill *H. pylori*, approximately the same concentration of bacteria. This could be an indication that a single AMP-ChMic is able to interact and kill at least one bacterium, demonstrating the usefulness of the use of small ChMic diameters. The bactericidal properties of AMP-ChMic seem to derive from the immobilized MSI-78A-SH on its surface. These are preliminary results and more assays have to be done to prove this theory, namely with the same concentrations for ChMic', PEG-ChMic, and AMP-ChMic, which was not possible in the abovementioned assay, due to the lack of sufficient ChMic' and PEG-ChMic. After 30 minutes of incubation with the controls, there was a decrease of viable bacteria, however, in the following time points, 2 and 6 h, the numbers increased, surpassing even *H. pylori*. It is a possibility that exposing bacteria for longer periods of time, namely 24 h, but to lower concentrations, can also promote *H. pylori* killing. This hypothesis takes particular importance when considering possible cytotoxicity, as lower amounts of AMP-ChMic would reduce it. It is important to highlight the bactericidal effect of the AMP-ChMic, as within 30 min, they were able to reduce the bacterial load in 4 CFU logs.

One of the aims of this bioengineered strategy was to reduce the amount of AMP needed to have a bactericidal effect when compared with a drug delivery system (MSI-78A encapsulated), or to the MSI-78A in free solution. The MIC of MSI-78A was reported to be 8 and 16 μg/mL for *H. pylori* ATCC43526 and ATCC43579, respectively [8]. So far, the obtained results point that the quantity of AMP used to induce killing is still high, 62 μg/mL, as big concentrations of AMP-ChMic were used. However, it is important to stress that these are preliminary results and serve as a proof-of-concept to demonstrate the efficacy of AMP-ChMic, corroborated by the highly pathogenicity and virulence of the *H. pylori* strain selected. In the future, as this strategy is further optimized, it is expected to use smaller AMP-ChMic concentrations and still achieve the same antibacterial performance. Nevertheless, these first results give a strong indication that AMP-ChMic may be an effective non-antibiotic based strategy targeting *H. pylori*.

Chapter 6

General Conclusions and Future Perspectives

H. pylori infection affects more than 50 % of the population worldwide, 4.4 billion people [29], and is the cause of several gastric diseases that can lead to gastric cancer [2]. To date, the available therapies to eradicate *H. pylori* infection rely on the conjugation of two or more antibiotics with a proton pump inhibitor [4]. These therapies have had their efficacy rates decreasing to values lower than 80 %, considered unacceptable by the Maastricht V/Florence consensus [4]. As current treatments cannot deliver the expected outcome, it is crucial to develop new strategies to fight this gastric pathogen.

Bioengineered strategies present themselves as a revolutionary tool to improve several problems related to the current antibiotic based treatment regimens. The main goal of this dissertation was the development of an antibiotic-free bioengineered strategy to fight *H. pylori* infection. This strategy comprised a ChMic with an immobilized antimicrobial peptide that was previously reported as having anti-*H. pylori* effect. Microspheres were produced within the size range desired, 2 to 7 µm, to be approximately the same size as the bacteria and enhance a one-to one interaction. Microspheres also demonstrated to be suitable for acidic conditions, as their integrity was not affected in low pH. MSI-78A-SH immobilization on ChMic was successfully achieved with a high yield, attesting the effectiveness of the selected immobilization chemistry. The obtained AMP-ChMic showed a fast bactericidal effect against *H. pylori* in a concentration dependent way, with significant bacterial load reduction after 30 min (with concentrations around 10^5 µg/mL in PBS and 10^7 µg/mL in bacterial medium), proving its potential to act as alternative to commonly used therapies. Moreover, this strategy was also able to kill *H. pylori* in coccoid form, a more resistant state of bacteria, as suggested by PBS assays.

The AMP-ChMic strategy proposed in this dissertation are a novelty, as to date and to the best of our knowledge, only one study has been published using an AMP delivery system to fight *H. pylori* infection [100]. However, this study uses a different strategy (microspheres for AMP gastric delivery) and a different AMP (MSI-78 instead of MSI-78A, being the later more active against *H. pylori*).

The AMP-ChMic herein presented are an interesting approach targeting *H. pylori* infection. Firstly, as theoretically immobilization prevents AMP aggregation, it would allow the use of small quantities of the peptide, overcoming traditional drawbacks associated to AMP. Then, their mechanism of action is thought to be by interaction with the cell membrane, which makes it difficult for the bacteria to acquire resistance [19]. It is also important to emphasize the small size of the designed microspheres, which is approximately the same as *H. pylori* size. This feature is thought to allow a close contact between bacteria and the immobilized MSI-78A-SH on microsphere surface, and possible ability for one single particle to kill more than one bacterium. Moreover and more importantly, these microspheres do not rely on an antibiotic to exert a bactericidal effect.

The promising results obtained demonstrate the potential of AMP-ChMic as a novel strategy to overcome *H. pylori* infection. However, further studies need to be carried out to consolidate this strategy and bring it onto “real-world” applications.

An important aspect that should be further studied is the cytotoxicity of these AMP-ChMic. To evaluate the AMP-ChMic cytotoxicity, the modified Mic will be incubated with a gastric cell line, namely the gastric carcinoma cell line, MKN45 [111], and the AGS, human gastric adenocarcinoma cell [96]. Then, cells metabolic activity can be assessed by the resazurin assay. In order to be considered safe and biocompatible, AMP-ChMic cannot induce more than 30% cell lysis when using a direct contact assay, as stated in the international standard ISO 10993-5 [144].

Also, in this work, only AMP immobilization through the C-terminal was tested, however it would be interesting to see the effect of the orientation of MSI-78A-SH, and its relation with anti-*H. pylori* effect. It would be important to study if immobilization of the MSI-78A-SH by the N-terminal would significantly impact the overall bactericidal effect, since Costa *et al.* has previously demonstrated that based on the terminal by which AMP was immobilized it would led to different properties [145].

The AMP-ChMic proved to be resistant in a stomach-like acidic pH, however, to increase the resemblance with the actual gastric environment, the effect of enzymatic degradation should also be assessed. For that, incubation under simulated gastric fluid with pepsin, should be performed, as this is the most important enzyme present in the gastric juice and responsible for peptide bonds degradation [146]. Since the designed microspheres have an AMP exposed on its surface, this assay would allow to confirm that the immobilization process leads to less vulnerability to degradation by enzymatic cleavage.

A possible drawback of these AMP-ChMic is their non-specificity to *H. pylori*, meaning that it can kill other bacteria from the gastro-intestinal microbiota. To discard this hypothesis, screening assays will have to be performed with other gastro-intestinal bacteria, such as *Lactobacillus casei* and *Escherichia coli* to evaluate the AMP-ChMic bactericidal effect onto these bacteria [147]. Theoretically, the specificity problem can be overcome by adding to the AMP-ChMic specific receptors towards *H. pylori* adhesins [5,6].

After performing the above-mentioned assays to further validate this strategy, *in vivo* assays must be performed. For that, *H. pylori* SS1 strain, which is capable of infecting mice [148], should be assayed with the AMP-ChMic, to ensure that similar results to those previous obtained with *H. pylori* J99 (human strain). After performing this checkpoint, *in vivo* assays could be performed in C57BL/6 mouse strain, establishing *H. pylori* infection in this animal model and then designing an adequate protocol for dosage, administration route and effectiveness in infection eradication assays. Even though not being the optimal animal model, as mice are not naturally infected by *H. pylori* [149] like pigs are, it is the established model in the institute, and would still provide valuable information about the performance of the AMP-ChMic in a living organism.

Also, storage under different temperature conditions and time length is an important aspect to evaluate in the near future.

With this work, a step further has been taken regarding the state of the art of antibiotic-free alternatives to *H. pylori* current therapies. AMP-ChMic are an easy strategy to produce in a large scale, as its production is simple, fast and large-scale production would meet cost effectiveness demands. Furthermore, their non-dependence of antibiotics comes to meet the need to develop antibiotic-free therapies in the 21st century, as the antibiotic era initiated in the 19th century comes to an end. Further developing this strategy for establishing it as a safe therapeutic regimen would positively impact the life of millions of people worldwide.

References

[1] N. Almeida *et al.*, “Helicobacter pylori antimicrobial resistance rates in the central region of Portugal,” *Clin. Microbiol. Infect.*, vol. 20, no. 11, pp. 1127–1133, 2014.

[2] R. M. Peek and M. J. Blaser, “Helicobacter pylori and gastrointestinal tract adenocarcinomas,” *Nat. Rev. Cancer*, vol. 2, no. 1, pp. 28–34, 2002.

[3] “Cancer Key facts.” [Online]. Available: http://www.who.int/news-room/fact-sheets/detail/cancer. [Accessed: 31-Aug-2018].

[4] P. Malfertheiner *et al.*, “Management of helicobacter pylori infection-the Maastricht V/Florence consensus report,” *Gut*, vol. 66, no. 1, pp. 6–30, 2016.

[5] R. B. Umamaheshwari, S. Jain, D. Bhadra, and N. K. Jain, “Floating microspheres bearing acetohydroxamic acid for the treatment of Helicobacter pylori,” *J. Pharm. Pharmacol.*, vol. 55, no. 12, pp. 1607–1613, 2003.

[6] M.-D. Seo, H.-S. Won, J.-H. Kim, T. Mishig-Ochir, and B.-J. Lee, “Antimicrobial Peptides for Therapeutic Applications: A Review,” *Molecules*, vol. 17, no. 12, pp. 12276–12286, 2012.

[7] P. Parreira, M. Duarte, C. Reis, and M. C. L. Martins, “Helicobacter pylori infection: A brief overview on alternative natural treatments to conventional therapy,” *Crit. Rev. Microbiol.*, vol. 42, no. 1, pp. 94–105, 2016.

[8] A. Iwahori *et al.*, “On the Antibacterial Activity of Normal and Reversed Magainin 2 Analogs against Helicobacter pylori.,” *Biol. Pharm. Bull.*, vol. 20, no. 7, pp. 805–8, 1997.

[9] Z. Jing *et al.*, “Design and evaluation of novel pH-sensitive ureido-conjugated chitosan / TPP nanoparticles targeted to Helicobacter pylori,” *Biomaterials*, vol. 84, pp. 276-285, 2016.

[10] B. J. Marshall and J. R. Warren, “Unidentified curved bacilli in the stomach of patient with gastritits and peptic ulceration,” *Lancet*, vol. 8390, pp. 1311–1314, 1984.

[11] T. L. Cover and M. J. Blaser, “Helicobacter pylori and gastroduodenal disease,” *Annu. Rev. Med.*, vol. 43, pp. 135–145, 1992.

[12] C. Stewart Goodwin *et al.*, “Transfer of Campylobacter pylori and Campylobacter mustelae to Helicobacter gen.nov.as Helicobacter pylori comb.nov. and Helicobacter mustelae comb.nov., respectively.,” *Int. J. Syst. Bacteriol.*, vol. 39, no. 4, pp. 397–405, 1989.

[13] L. E. Wroblewski, R. M. P. Jr, T. Keith, L. E. Wroblewski, R. M. Peek, and K. T. Wilson, “Helicobacter pylori and Gastric Cancer : Factors That Modulate Disease Risk Helicobacter pylori and Gastric Cancer : Factors That Modulate Disease Risk,” *Clin. Microbiol. Rev.*, vol. 23, no. 4, pp. 713–739, 2010.

[14] “Schistosomes, liver flukes and Helicobacter pylori. IARC Working Group on the Evaluation of Carcinogenic Risks to Humans. Lyon, 7-14 June 1994.”

[15] B. N. Dang and D. Y. Graham, “Helicobacter pylori infection and antibiotic resistance: a WHO high priority?,” *Nat. Rev. Gastroenterol. Hepatol.*, vol. 14, no. 7, pp. 383-384, 2017.

[16] C. Dunne, B. Dolan, and M. Clyne, “Helicobacter pylori Factors that mediate colonization of the human stomach by,” *World J. Gastroenterol.*, vol. 20, no. 19, pp. 5610–5624, 2014.

[17] J. G. Kusters, A. H. M. van Vliet, and E. J. Kuipers, “Pathogenesis of Helicobacter pylori Infection,” *Clin. Microbiol. Rev.*, vol. 19, no. 3, pp. 449–490, 2006.

[18] Y. Khosravi, Y. Dieye, M. F. Loke, K. L. Goh, and J. Vadivelu, “Streptococcus mitis

induces conversion of helicobacter pylori to coccoid cells during co-culture in vitro," *PLoS One*, vol. 9, no. 11, pp. 1–11, 2014.

[19] P. W. O' Toole, M. C. Lane, and S. Porwollik, "Helicobacter pylori motility," *Microbes Infect.*, vol. 2, no. 10, pp. 1207–1214, 2000.

[20] K. A. Eaton, D. R. Morgan, and S. Krakowka, "Campylobacter pylori virulence factors in gnotobiotic piglets," *Infect. Immun.*, vol. 57, pp. 1119–1125, 1989.

[21] K. A. Eaton, S. Suerbaum, C. Josenhans, and S. Krakowka, "Colonization of gnotobiotic piglets by Helicobacter pylori deficient in two flagellin genes," *Infect. Immun.*, vol. 64, no. 7, pp. 2445–2448, 1996.

[22] F. P. Douillard *et al.*, "The HP0256 gene product is involved in motility and cell envelope architecture of Helicobacter pylori.," *BMC Microbiol.*, vol. 10, p. 106, 2010.

[23] C.-Y. Kao, B.-S. Sheu, and J.-J. Wu, "Helicobacter pylori infection: An overview of bacterial virulence factors and pathogenesis," *Biomed. J.*, vol. 39, no. 1, pp. 14–23, 2016.

[24] S. Schreiber *et al.*, "Rapid Loss of Motility of Helicobacter pylori in the Gastric Lumen In Vivo Rapid Loss of Motility of Helicobacter pylori in the Gastric Lumen In Vivo So," *Infect. Immun.*, vol. 73, no. 3, pp. 1–7, 2005.

[25] P. Parreira, A. Magalhães, C. A. Reis, T. Borén, D. Leckband, and M. C. L. Martins, "Bioengineered surfaces promote specific protein – glycan mediated binding of the gastric pathogen Helicobacter pylori," *Acta Biomater.*, vol. 9, no. 11, pp. 8885–8893, 2013.

[26] M. Oleastro and A. Ménard, "The Role of Helicobacter pylori Outer Membrane Proteins in Adherence and Pathogenesis," *Biology (Basel).*, vol. 2, pp. 1110–1134, 2013.

[27] J. Atherton, "The pathogenesis of Helicobacter pylori-induced gastro-duodenal diseases," *Annu Rev Pathol.*, vol. 1, pp. 63–96, 2006.

[28] H. M. Algood and T. L. Cover, "Helicobacter pylori persistence: an overview of interactions between H. pylori and host immune defenses," *Clin. Microbiol. Rev.*, vol. 19, no. 4, pp. 597–613, 2006.

[29] J. K. Y. Hooi *et al.*, "Global Prevalence of Helicobacter pylori Infection: Systematic Review and Meta-Analysis," *Gastroenterology*, vol. 153, no. 2, pp. 420–429, 2017.

[30] B. Peleteiro, A. Bastos, A. Ferro, and N. Lunet, "Prevalence of Helicobacter pylori infection worldwide: A systematic review of studies with national coverage," *Dig. Dis. Sci.*, vol. 59, no. 8, pp. 1698–1709, 2014.

[31] C. Burucoa and A. Axon, "Epidemiology of *Helicobacter pylori* infection," *Helicobacter*, vol. 22, no. S1, p. e12403, 2017.

[32] L. M. Brown, "Helicobacter pylori: epidemiology and routes of transmission," *Epidemiol. Rev.*, vol. 22, no. 2, pp. 283–297, 2000.

[33] P. Malfertheiner *et al.*, "Management of Helicobacter pylori infection d the Maastricht IV / Florence Consensus Report," *Gut*, vol. 61, pp. 646–664, 2012.

[34] T. L. Testerman and J. Morris, "Beyond the stomach : An updated view of Helicobacter pylori pathogenesis , diagnosis , and treatment," *World J. Gastroenterol.*, vol. 20, no. 36, pp. 12781–12808, 2014.

[35] W. D. Chey and B. C. Y. Wong, "American College of Gastroenterology Guideline on the Management of Helicobacter pylori Infection," *Am. J. Gastroenterol.*, vol. 102, no. 8, pp. 1808–1825, 2007.

[36] C. A. Fallone *et al.*, "The Toronto Consensus for the Treatment of Helicobacter pylori Infection in Adults," *Gastroenterology*, 2016.

[37] J. Heo and S. W. Jeon, "Optimal treatment strategy for Helicobacter pylori: Era of antibiotic resistance," *World J. Gastroenterol.*, vol. 20, no. 19, pp. 5654–5659, 2014.

[38] S. M. Campo, A. Zullo, C. Hassan, and S. Morini, "Antibiotic treatment strategies for Helicobacter pylori infection," *Recent Pat Antiinfect Drug Discov.*, vol. 2, no. 1, pp. 11–7, 2007.

[39] D. Lopes, C. Nunes, M. C. L. Martins, B. Sarmento, and S. Reis, "Eradication of Helicobacter pylori: Past, present and future," *J. Control. Release*, vol. 189, pp. 169–186, 2014.

[40] V. Ricci, R. Zarrilli, and M. Romano, "Voyage of Helicobacter pylori in human stomach: odyssey of a bacterium," *Dig Liver Dis.*, vol. 34, no. 1, pp. 2–8, 2002.

[41] R. Ghotaslou, H. E. Leylabadlo, and Y. M. Asl, "Prevalence of antibiotic resistance in

Helicobacter pylori : A recent literature review," *World J Methodol*, vol. 5, no. 3, pp. 164–174, 2015.

[42] V. De Francesco *et al.*, "Worldwide H . pylori Antibiotic Resistance : a Systematic Review," *J Gastrointestin Liver Dis.*, vol. 19, no. 4, pp. 409–414, 2010.

[43] K. E. L. McColl, "Helicobacter pylori infection.," *N. Engl. J. Med.*, vol. 362, no. 17, pp. 1597–1604, 2010.

[44] E. L. Silva-Freitas *et al.*, "Design of Magnetic Polymeric Particles as a Stimulus-Responsive System for Gastric Antimicrobial Therapy," *AAPS PharmSciTech*, vol. 18, no. 6, pp. 2026–2036, 2016.

[45] D. Zhou *et al.*, "Preparation and Characterization of a Novel pH-Sensitive Coated Microsphere for Duodenum-Specific Drug Delivery," *Arch Pharm Res*, vol. 35, no. 5, pp. 839–850, 2012.

[46] D. Velin, K. Straubinger, and M. Ge, "Inflammation, immunity, and vaccines for Helicobacter pylori infection," *Helicobacter*, vol. 21, no. 1, pp. 26–29, 2016.

[47] P. Sutton, "Progress in vaccination against Helicobacter pylori," *Vaccine*, vol. 19, no. 17, pp. 2286–2290, 2001.

[48] T. G. Blanchard, "Current Status and Prospects for a Helicobacter pylori Vaccine," *Gastroenterol Clin N Am*, vol. 44, no. 3, pp. 677–689, 2015.

[49] P. Michetti *et al.*, "Oral immunization with urease and Escherichia coli heat-labile enterotoxin is safe and immunogenic in Helicobacter pylori-infected adults.," *Gastroenterology*, vol. 116, no. 4, pp. 804–812, 1999.

[50] H. Angelakopoulos and E. L. Hohmann, "Pilot study of phoP/phoQ-deleted Salmonella enterica serovar typhimurium expressing Helicobacter pylori urease in adult volunteers.," *Infect. Immun.*, vol. 68, no. 4, pp. 2135–2141, 2000.

[51] K. L. Kotloff, M. B. Sztein, S. S. Wasserman, G. A. Losonsky, S. C. DiLorenzo, and R. I. Walker, "Safety and immunogenicity of oral inactivated whole-cell Helicobacter pylori vaccine with adjuvant among volunteers with or without subclinical infection.," *Infect. Immun.*, vol. 69, no. 6, pp. 3581–3590, 2001.

[52] D. Bumann *et al.*, "Safety and immunogenicity of live recombinant Salmonella enterica serovar Typhi Ty21a expressing urease A and B from Helicobacter pylori in human volunteers.," *Vaccine*, vol. 20, no. 5–6, pp. 845–852, 2001.

[53] S. Sougioultzis *et al.*, "Safety and efficacy of E coli enterotoxin adjuvant for urease-based rectal immunization against Helicobacter pylori.," *Vaccine*, vol. 21, no. 3–4, pp. 194–201, 2002.

[54] W. G. Metzger *et al.*, "Impact of vector-priming on the immunogenicity of a live recombinant Salmonella enterica serovar typhi Ty21a vaccine expressing urease A and B from Helicobacter pylori in human volunteers.," *Vaccine*, vol. 22, no. 17–18, pp. 2273–2277, 2004.

[55] T. Aebischer *et al.*, "Correlation of T cell response and bacterial clearance in human volunteers challenged with Helicobacter pylori revealed by randomised controlled vaccination with Ty21a-based Salmonella vaccines.," *Gut*, vol. 57, no. 8, pp. 1065–1072, 2008.

[56] P. Malfertheiner *et al.*, "Safety and immunogenicity of an intramuscular Helicobacter pylori vaccine in noninfected volunteers: a phase I study.," *Gastroenterology*, vol. 135, no. 3, pp. 787–795, 2008.

[57] Zeng M *et al.*, "Efficacy, safety, and immunogenicity of an oral recombinant Helicobacter pylori vaccine in children in China: a randomised, double-blind, placebo-controlled, phase 3 trial," *Lancet.*, vol. 386, pp. 1457–1464, 2015.

[58] F. Anderl and M. Gerhard, "Helicobacter pylori vaccination: Is there a path to protection?," *World J. Gastroenterol.*, vol. 20, no. 34, pp. 11939–11949, 2014.

[59] FAO/WHO, "Guidelines for the evaluation of probiotics in food. Report of a joint FAO/WHO working group on drafting guidelines for the evaluation of probiotics in food," 2000.

[60] G. Ayala, W. I. Escobedo-hinojosa, C. F. De Cruz-herrera, and I. Romero, "Exploring alternative treatments for Helicobacter pylori infection," *World J. Gastroenterol.*, vol. 20, no. 6, pp. 1450–1469, 2014.

[61] L. Pacifico, J. F. Osborn, E. Bonci, S. Romaggioli, R. Baldini, and C. Chiesa, "Probiotics for the treatment of Helicobacter pylori infection in children," *World J Gastroenterol.*,

vol. 20, no. 3, pp. 673–683, 2014.

[62] A. L. Servin, “Antagonistic activities of lactobacilli and bifidobacteria against microbial pathogens,” *FEMS Microbiol. Rev.*, vol. 28, no. 4, pp. 405–440, 2004.

[63] A. Patel, N. Shah, and J. B. Prajapati, “Clinical application of probiotics in the treatment of Helicobacter pylori infectiond-A brief review,” *J. Microbiol. Immunol. Infect.*, vol. 47, pp. 429–437, 2014.

[64] F. F. Vale and M. Oleastro, “Overview of the phytomedicine approaches against Helicobacter pylori,” *World J Gastroenterol.*, vol. 20, no. 19, pp. 5594–5609, 2014.

[65] Y.-C. Wang, “Medicinal plant activity on Helicobacter pylori related diseases,” *World J Gastroenterol.*, vol. 20, no. 30, pp. 10368–10382, 2014.

[66] Y. C. Wang, D. C. Wu, J. J. Liao, C. H. Wu, W. Y. Li, and B. C. Weng, “In vitro activity of Impatiens balsamina L. against multiple antibiotic-resistant Helicobacter pylori,” *Am J Chin Med*, vol. 37, pp. 713–722, 2009.

[67] Y. C. Wang *et al.*, “In vitro activity of 2-methoxy-1,4-naphthoquinone and stigmasta-7,22-diene-3ß-ol from impatiens balsamina L. against multiple antibiotic-resistant Helicobacter pylori,” *Evid Based Complement Altern. Med*, vol. 2011, 2011.

[68] C. Njume, A. J. Afolayan, E. Green, and R. N. Ndip, “Volatile compounds in the stem bark of Sclerocarya birrea (Anacardiaceae) possess antimicrobial activity against drug-resistant strains of Helicobacter pylori,” *Int J Antimicrob Agents*, vol. 38, pp. 319–324, 2011.

[69] N. Hamasaki *et al.*, “Highly selective antibacterial activity of novel alkyl quinolone alkaloids from a Chinese herbal medicine, Gosyuyu (Wu-Chu-Yu), against Helicobacter pylori in vitro,” *Microbiol Immunol*, vol. 44, pp. 9–15, 2000.

[70] H. Takeuchi, V. T. Trang, N. Morimoto, Y. Nishida, Y. Matsumura, and T. Sugiura, “Natural products and food components with anti-Helicobacter pylori activities,” *World J Gastroenterol.*, vol. 20, no. 27, pp. 8971–8978, 2014.

[71] F. Costa, I. F. Carvalho, R. C. Montelaro, P. Gomes, and M. C. L. Martins, “Covalent immobilization of antimicrobial peptides (AMPs) onto biomaterial surfaces,” *Acta Biomater.*, vol. 7, no. 4, pp. 1431–1440, 2011.

[72] W. Van ’T Hof, E. C. I. Veerman, E. J. Heimerhorst, and A. V. Nieuw Amerongen, “Antimicrobial peptides: Properties and applicability,” *Biol. Chem.*, vol. 382, no. 4, pp. 597–619, 2001.

[73] L. Zhang *et al.*, “Cathelicidin protects against Helicobacter pylori colonization and the associated gastritis in mice.,” *Gene Ther.*, vol. 20, no. 7, pp. 751–760, 2013.

[74] L. Zhang *et al.*, “Critical Role of Antimicrobial Peptide Cathelicidin for Controlling Helicobacter pylori Survival and Infection.,” *J Immunol.*, vol. 196, no. 4, pp. 1799–1809, 2016.

[75] M. M. Rigano *et al.*, “A novel synthetic peptide from a tomato defensin exhibits antibacterial activities against Helicobacter pylori,” *J. Pept. Sci.*, vol. 18, no. 12, pp. 755–762, 2012.

[76] Y. Ge, D. L. Macdonald, K. J. Holroyd, C. Thornsberry, H. Wexle, and M. Zasloff, “In Vitro Antibacterial Properties of Pexiganan , an Analog of Magainin,” *Antimicrob. Agents Chemother.*, vol. 43, no. 4, pp. 782–788, 1999.

[77] L. Chen, Y. Li, J. Li, X. Xu, R. Lai, and Q. Zou, “An antimicrobial peptide with antimicrobial activity against Helicobacter pylori,” vol. 28, pp. 1527–1531, 2007.

[78] M. O. Makobongo, T. Kovachi, H. Gancz, A. Mor, and D. S. Merrell, “In vitro antibacterial activity of acyl-lysyl oligomers against Helicobacter pylori,” *Antimicrob. Agents Chemother.*, vol. 53, no. 10, pp. 4231–4239, 2009.

[79] J. L. Narayana, H.-N. Huang, C.-J. Wu, and J.-Y. Chen, “Efficacy of the antimicrobial peptide TP4 against Helicobacter pylori infection: in vitro membrane perturbation via micellization and in vivo suppression of host immune responses in a mouse model,” *Biomaterials*, vol. 61, no. 15, pp. 41–51, 2015.

[80] J. L. Narayana, H. N. Huang, C. J. Wu, and J. Y. Chen, “Epinecidin-1 antimicrobial activity: In vitro membrane lysis and In vivo efficacy against Helicobacter pylori infection in a mouse model,” *Biomaterials*, vol. 61, pp. 41–51, 2015.

[81] X. Wang *et al.*, “A new family of antimicrobial peptides from skin secretions of Rana pleuraden,” *Peptides*, vol. 28, no. 10, pp. 2069–2074, 2007.

[82] I. C. Gonçalves, P. C. Henriques, C. L. Seabra, and M. C. L. Martins, “The potential

utility of chitosan micro / nanoparticles in the treatment of gastric infection," *Expert Rev Anti Infect Ther*, vol. 12, no. 8, pp. 981–992, 2014.

[83] L. Bi *et al.*, "Effects of different cross-linking conditions on the properties of genipin-cross-linked chitosan/collagen scaffolds for cartilage tissue engineering," *J. Mater. Sci. Mater. Med.*, vol. 22, no. 1, pp. 51–62, 2011.

[84] D. Suzuki *et al.*, "Comparison of various mixtures of β-chitin and chitosan as a scaffold for three-dimensional culture of rabbit chondrocytes," *J. Mater. Sci. Mater. Med.*, vol. 19, no. 3, pp. 1307–1315, 2008.

[85] I. A. Sogias, A. C. Williams, and W. Khutoryanskiy, "Why is chitosan mucoadhesive?," *Biomacromolecules*, vol. 9, no. 7, pp. 1837–1842, 2008.

[86] M. J. Moura, M. M. Figueiredo, and M. H. Gil, "Rheological study of genipin cross-linked chitosan hydrogels," *Biomacromolecules*, vol. 8, no. 12, pp. 3823–3829, 2007.

[87] J. Jin, M. Song, and D. J. Hourston, "Novel chitosan-based films cross-linked by genipin with improved physical properties," *Biomacromolecules*, vol. 5, no. 1, pp. 162–168, 2004.

[88] F. Nogueira, I. C. Gonçalves, and M. C. L. Martins, "Effect of gastric environment on Helicobacter pylori adhesion to a mucoadhesive polymer.," *Acta Biomater.*, vol. 9, no. 2, pp. 5208–15, 2013.

[89] J. Rhoades and S. Roller, "Antimicrobial actions of degraded and native chitosan against spoilage organisms in laboratory media and foods," *Appl. Environ. Microbiol.*, vol. 66, no. 1, pp. 80–86, 2000.

[90] D. Luo, J. Guo, and F. Wang, "Preparation and Evaluation of Anti-Helicobacter pylori Efficacy of Chitosan Nanoparticles in Vitro and in Vivo," *J. Biomater. Sci.*, vol. 20, no. 11, pp. 1587–1596, 2009.

[91] Y. Lin, C. Chang, Y. Wu, Y. Hsu, S. Chiou, and Y. Chen, "Development of pH-responsive chitosan / heparin nanoparticles for stomach-specific anti- Helicobacter pylori therapy," *Biomaterials*, vol. 30, no. 19, pp. 3332–3342, 2009.

[92] Y. Li, H. Y. Wang, and C. H. Cho, "Association of Heparin with Basic Fibroblast Growth Factor, Epidermal Growth Factor, and Constitutive Nitric Oxide Synthase on Healing of Gastric Ulcer in Rats," *J. Pharmacol. Exp. Ther.*, vol. 290, no. 2, pp. 789–796, 1999.

[93] F. L. Mi, Y. C. Tan, H. C. Liang, R. N. Huang, and H. W. Sung, "In vitro evaluation of a chitosan membrane cross-linked with genipin," *J Biomater Sci Polym Ed.*, vol. 12, no. 8, pp. 835–850, 2001.

[94] M. Fernandes, I. C. Gonçalves, S. Nardecchia, I. F. Amaral, M. A. Barbosa, and M. C. L. Martins, "Modulation of stability and mucoadhesive properties of chitosan microspheres for therapeutic gastric application," *Int. J. Pharm.*, vol. 454, no. 1, pp. 116–124, 2013.

[95] I. C. Gonçalves, A. Magalhães, M. Fernandes, I. V Rodrigues, C. A. Reis, and M. C. L. Martins, "Bacterial-binding chitosan microspheres for gastric infection treatment and prevention," *Acta Biomater.*, vol. 9, no. 12, pp. 9370–9378, 2013.

[96] I. C. Gonçalves *et al.*, "Bacteria-targeted biomaterials : Glycan-coated microspheres to bind Helicobacter pylori," *Acta Biomater.*, vol. 33, pp. 40–50, 2016.

[97] Y. Lin, C. Feng, C. Lai, J. Lin, and H. Chen, "Preparation of epigallocatechin gallate-loaded nanoparticles and characterization of their inhibitory effects on Helicobacter pylori growth in vitro and in vivo," *Sci. Technol. Adv. Mater.*, vol. 15, 2014.

[98] K. Mabe, M. Yamada, I. Oguni, and T. Takahashi, "In Vitro and In Vivo Activities of Tea Catechins against Helicobacter pylori," *Antimicrob Agents Chemother*, vol. 43, no. 7, pp. 1788–1791, 1999.

[99] Y.-K. Yee and M. W.-L. Koo, "Anti-Helicobacter pylori activity of Chinese tea: in vitro study," *Aliment Pharmacol Ther*, vol. 14, pp. 635–638, 2000.

[100] Y.-H. Lin *et al.*, "Berberine-loaded targeted nanoparticles as specific Helicobacter pylori eradication therapy : in vitro and in vivo study," *Nanomedicine*, vol. 10, no. 1, pp. 57–71, 2015.

[101] C. Chang *et al.*, "Development of novel nanoparticles shelled with heparin for berberine delivery to treat Helicobacter pylori," *Acta Biomater.*, vol. 7, no. 2, pp. 593–603, 2011.

[102] X. Zhang *et al.*, "The Synthetic Antimicrobial Peptide Pexiganan and Its Nanoparticles (PNPs) Exhibit the Anti-Helicobacter pylori Activity in Vitro and in Vivo," *Molecules*, vol. 20, pp. 3972–3985, 2015.

[103] R. B. Umamaheshwari and N. K. Jain, "Receptor Mediated Targeting of Lectin

Conjugated Gliadin Nanoparticles in the Treatment of Helicobacter pylori," *J. Drug Target.*, vol. 11, no. 7, pp. 415–424, 2003.
[104] M. M. Khin, J. S. Hua, H. C. Ng, T. Wadstrom, and H. Bow, "Agglutination of Helicobacter pylori coccoids by lectins.," *World J Gastroenterol.*, vol. 6, no. 2, pp. 202–209, 2000.
[105] R. B. Umamaheshwari and N. K. Jain, "Receptor-mediated targeting of lipobeads bearing acetohydroxamic acid for eradication of Helicobacter pylori," *J. Control. Release*, vol. 99, no. 1, pp. 27–40, 2004.
[106] C.A. Lingwood, M. Huessca, and A. Kuksis, "The glycerolipid receptor for Helicobacter pylori (and Exoenzyme S) is phosphatidyl ethanolamine," *Infect. Immun.*, no. 60, pp. 2470–2476, 1992.
[107] S. W. Jung and S. W. Lee, "The antibacterial effect of fatty acids on Helicobacter pylori infection.," *Korean J. Intern. Med.*, vol. 31, no. 1, pp. 30–5, 2016.
[108] M. Obonyo, L. Zhang, S. Thamphiwatana, D. Pornpattananangkul, V. Fu, and L. Zhang, "Antibacterial activities of liposomal linolenic acids against antibiotic-resistant Helicobacter pylori," *Mol. Pharm.*, vol. 9, no. 9, pp. 2677–2685, 2012.
[109] S. Thamphiwatana, W. Gao, M. Obonyo, and L. Zhang, "In vivo treatment of *Helicobacter pylori* infection with liposomal linolenic acid reduces colonization and ameliorates inflammation," *Proc. Natl. Acad. Sci.*, vol. 111, no. 49, pp. 17600–17605, 2014.
[110] S. W. Jung, S. Thamphiwatana, L. Zhang, and M. Obonyo, "Mechanism of antibacterial activity of liposomal linolenic acid against helicobacter pylori," *PLoS One*, vol. 10, no. 3, pp. 1–13, 2015.
[111] C. L. Seabra *et al.*, "Docosahexaenoic acid loaded lipid nanoparticles with bactericidal activity against Helicobacter pylori," *Int. J. Pharm.*, vol. 519, no. 1–2, pp. 128–137, 2017.
[112] K. Naik and M. Kowshik, "The silver lining: towards the responsible and limited usage of silver," *J. Appl. Microbiol.*, vol. 123, pp. 1068–1087, 2017.
[113] M. Amin, F. Anwar, M. Ramzan, and S. Ashraf, "Green Synthesis of Silver Nanoparticles through Reduction with Solanum xanthocarpum L . Berry Extract : Characterization , Antimicrobial and Urease Inhibitory Activities against Helicobacter pylori," *Int. J. Mol. Sci.*, vol. 13, pp. 9923–9941, 2012.
[114] M. Amin *et al.*, "Green Synthesis of Silver Nanoparticles : Structural Features and In Vivo and In Vitro Therapeutic Effects against Helicobacter pylori Induced Gastritis," *Bioinorg. Chem. Appl.*, vol. 2014, 2014.
[115] M. Amin *et al.*, "Mechanochemical synthesis and in vitro antiHelicobacter pylori and uresase inhibitory activities of novel zinc(II)-famotidine complex," *J. Enzyme Inhib. Med. Chem.*, vol. 25, no. 3, pp. 383–390, 2010.
[116] P. Pan-in, W. Banlunara, and S. Suksamrarn, "Combating Helicobacter pylori infections with mucoadhesive nanoparticles loaded with Garcinia mangostana extract," *Nanomedicine*, vol. 9, no. 3, pp. 457–468, 2012.
[117] X. Zhu, D. Zhou, Y. Jin, Y. P. Song, Z. R. Zhang, and Y. Huang, "A novel microsphere with a three-layer structure for duodenum-specific drug delivery," *Int. J. Pharm.*, vol. 413, no. 1–2, pp. 110–118, 2011.
[118] M. A. Khalil, M. M. El-Sheekh, H. I. El-Adawi, N. M. El-Deeb, and M. Z. Hussein, "Efficacy of microencapsulated lactic acid bacteria in helicobater pylori eradication therapy," *J. Res. Med. Sci.*, vol. 20, no. 10, pp. 950–957, 2015.
[119] A. Fulgione, N. Nocerino, M. Iannaccone, and S. Roperto, "Lactoferrin Adsorbed onto Biomimetic Hydroxyapatite Nanocrystals Controlling - In Vivo - the Helicobacter pylori Infection," *PLoS One*, vol. 11, no. 7, 2016.
[120] I. F. Amaral, P. L. Granja, and M. A. Barbosa, "Chemical modification of chitosan by phosphorylation: an XPS, FT-IR and SEM study," *J. Biomater. Sci.-Polym. Ed.*, vol. 16, pp. 1575–1593, 2005.
[121] B. N. Estevinho, F. Rocha, L. Santos, and A. Alves, "Microencapsulation with chitosan by spray drying for industry applications - A review," *Trends Food Sci. Technol.*, vol. 31, no. 2, pp. 138–155, 2013.
[122] J. Brugnerotto, J. Lizardi, F. M. Goycoolea, W. Argüelles-Monal, J. Desbrières, and M. Rinaudo, "An infrared investigation in relation with chitin and chitosan characterization," *Polymer (Guildf).*, vol. 42, no. 8, pp. 3569–3580, 2001.

[123] V. Rocha *et al.*, “In vitro cytotoxicity evaluation of resveratrol-loaded nanoparticles: Focus on the challenges of in vitro methodologies,” *Food Chem. Toxicol.*, vol. 103, pp. 214–222, 2017.

[124] C. Monteiro *et al.*, “Antimicrobial properties of membrane-active dodecapeptides derived from MSI-78,” *Biochim. Biophys. Acta - Biomembr.*, vol. 1848, no. 5, pp. 1139–1146, 2015.

[125] P. Parreira *et al.*, “Effect of surface chemistry on bacterial adhesion, viability, and morphology,” *J. Biomed. Mater. Res. - Part A*, vol. 99 A, no. 3, pp. 344–353, 2011.

[126] “CLSI. Performance Standards for Antimicrobial Susceptibility Testing; Twenty-Fifth Informational Supplement; 2015.”

[127] P. Parreira *et al.*, “Eucalyptus spp. outer bark extracts inhibit Helicobacter pylori growth: in vitro studies,” *Ind. Crops Prod.*, vol. 105, pp. 207–214, 2017.

[128] J. R. Oliveira, M. C. L. Martins, L. Mafra, and P. Gomes, “Synthesis of an O-alkynyl-chitosan and its chemoselective conjugation with a PEG-like amino-azide through click chemistry,” *Carbohydr. Polym.*, vol. 87, no. 1, pp. 240–249, 2012.

[129] G. Socrates, *Infrared and Raman Characteristic Group Frequencies: Tables and Charts*. Chichester, UK: Wiley, 2001.

[130] B. M. Espinosa-García, W. M. Argüelles-Monal, J. Hernández, L. Félix-Valenzuela, N. Acosta, and F. M. Goycoolea, “Molecularly imprinted Chitosan - Genipin hydrogels with recognition capacity toward o-Xylene,” *Biomacromolecules*, vol. 8, no. 11, pp. 3355–3364, 2007.

[131] R. Harris, E. Lecumberri, and A. Heras, “Chitosan-genipin microspheres for the controlled release of drugs: Clarithromycin, tramadol and heparin,” *Mar. Drugs*, vol. 8, no. 6, pp. 1750–1762, 2010.

[132] A. Sosnik and K. P. Seremeta, “Advantages and challenges of the spray-drying technology for the production of pure drug particles and drug-loaded polymeric carriers,” *Adv. Colloid Interface Sci.*, vol. 223, pp. 40–54, 2015.

[133] A. Gharsallaoui, G. Roudaut, O. Chambin, A. Voilley, and R. Saurel, “Applications of spray-drying in microencapsulation of food ingredients: an overview,” *Food Res. Int.*, vol. 40, no. 9, pp. 1107–1121, 2007.

[134] A. R. Lopes *et al.*, “Production of microparticles of molinate degrading biocatalysts using the spray drying technique,” *Chemosphere*, vol. 161, pp. 61–68, 2016.

[135] Y. L. Chang, T. C. Liu, and M. L. Tsai, “Selective Isolation of trypsin inhibitor and lectin from soybean whey by chitosan/tripolyphosphate/genipin co-crosslinked beads,” *Int. J. Mol. Sci.*, vol. 15, no. 6, pp. 9979–9990, 2014.

[136] F. Nogueira, I. C. Gonçalves, and M. C. L. Martins, “Effect of gastric environment on Helicobacter pylori adhesion to a mucoadhesive polymer,” *Acta Biomater.*, vol. 9, no. 2, pp. 5208–5215, 2013.

[137] L. C. Shriver-Lake, G. P. Anderson, and C. R. Taitt, “Effect of Linker Length on Cell Capture by Poly(ethylene glycol)-Immobilized Antimicrobial Peptides,” *Langmuir*, vol. 33, no. 11, pp. 2878–2884, 2017.

[138] X. Wu, P. H. Wei, X. Zhu, M. J. Wirth, A. Bhunia, and G. Narsimhan, “Effect of immobilization on the antimicrobial activity of a cysteine-terminated antimicrobial Peptide Cecropin P1 tethered to silica nanoparticle against E. coli O157:H7 EDL933,” *Colloids Surfaces B Biointerfaces*, vol. 156, pp. 305–312, 2017.

[139] F. Costa, S. Maia, J. Gomes, P. Gomes, and M. C. L. Martins, “Characterization of hLF1-11 immobilization onto chitosan ultrathin films, and its effects on antimicrobial activity,” *Acta Biomater.*, vol. 10, no. 8, pp. 3513–3521, 2014.

[140] L. Racine, G. Costa, E. Bayma-Pecit, I. Texier, and R. Auzély-Velty, “Design of interpenetrating chitosan and poly(ethylene glycol) sponges for potential drug delivery applications,” *Carbohydr. Polym.*, vol. 170, pp. 166–175, 2017.

[141] R. Sarroukh, E. Goormaghtigh, J. M. Ruysschaert, and V. Raussens, “ATR-FTIR: A ‘rejuvenated’ tool to investigate amyloid proteins,” *Biochim. Biophys. Acta - Biomembr.*, vol. 1828, no. 10, pp. 2328–2338, 2013.

[142] P. R. Marreco, P. Da Luz Moreira, S. C. Genari, and Â. M. Moraes, “Effects of different sterilization methods on the morphology, mechanical properties, and cytotoxicity of chitosan membranes used as wound dressings,” *J. Biomed. Mater. Res. - Part B Appl. Biomater.*, vol. 71, no. 2, pp. 268–277, 2004.

[143] R. M. Fernandes, H. Silva, R. Oliveira, C. Almeida, N. F. Azevedo, and M. J. Vieira, "Morphological transition of Helicobacter pylori adapted to water," *Future Microbiol.*, vol. 12, no. 13, pp. 1167–1179, 2017.
[144] "ISO10993-5, 2009. Part 5: tests for in vitro cytotoxicity, Biological Evaluation of Medical Devices. 3rd ed. International Organization for Standardization, Geneva, Switzerland."
[145] F. M. T. A. Costa, S. R. Maia, P. A. C. Gomes, and M. C. L. Martins, "Dhvar5 antimicrobial peptide (AMP) chemoselective covalent immobilization results on higher antiadherence effect than simple physical adsorption," *Biomaterials*, vol. 52, no. 1, pp. 531–538, 2015.
[146] R. J. C. Stewart, H. Morton, J. Coad, and K. C. Pedley, "*In vitro* digestion for assessing micronutrient bioavailability: the importance of digestion duration," *Int. J. Food Sci. Nutr.*, vol. 0, no. 0, pp. 1–7, 2018.
[147] C. L. Seabra *et al.*, "Lipid nanoparticles to counteract gastric infection without affecting gut microbiota," *Eur. J. Pharm. Biopharm.*, vol. 127, no. September 2017, pp. 378–386, 2018.
[148] S. Fontenete *et al.*, "Fluorescence in vivo hybridization (FIVH) for detection of helicobacter pylori infection in a C57BL/6 mouse model," *PLoS One*, vol. 11, no. 2, pp. 1–18, 2016.
[149] K. F. Boehnke, K. A. Eaton, M. Valdivieso, L. H. Baker, and C. Xi, "Animal Model Reveals Potential Waterborne Transmission of Helicobacter pylori Infection," *Helicobacter*, vol. 20, no. 5, pp. 326–333, 2015.